JEADV ISSN 1468-3083

CASE REPORT

Successful treatment of severe recalcitrant erosive oral lichen planus with topical tacrolimus

R Shichinohe, A Shibaki,* W Nishie, Y Tateishi, H Shimizu

Department of Dermatology, Hokkaido University Graduate School of Medicine, North 15 West 7, Kita-ku, Sapporo 060-8638, Japan.

Keywords
oral lichen planus, tacrolimus, topical treatment

*Corresponding author,
tel. +81 11 716 1161
ext. 5962; fax +81 11 706 7820;
E-mail: ashibaki@med.hokudai.ac.jp

Received: 29 March 2004, accepted 6 January 2005

DOI: 10.1111/j.1468-3083.2005.01338.x

Abstract

Oral lichen planus (LP) is a severe, painful form of LP, and is often resistant to topical corticosteroid therapy. Recently, open trials demonstrated that topical tacrolimus therapy was effective for the treatment of chronic erosive oral LP. We report two cases with severe recalcitrant erosive oral LP, who dramatically benefited from topical tacrolimus therapy. In case 1, a 64-year-old man presented with a 5-month history of painful erosions on his entire lower lip and buccal mucosa. Physical and histological examination confirmed a diagnosis of LP. He experienced rapid relief from pain and a dramatic improvement was obtained within 5 weeks of topical tacrolimus treatment. No significant irritation was observed and blood tacrolimus level was kept within a safe level (2.5 ng/mL). In case 2, a 68-year-old man developed painful erosions on his right lower lip and buccal mucosa 2 months before his arrival at our hospital. Histopathological analysis confirmed a diagnosis of oral LP. He experienced a rapid dramatic improvement of both lesions within 4 weeks of the start of tacrolimus application. No significant irritation or recurrence was observed. Thus, topical tacrolimus is suggested as a well-tolerated, effective therapy for oral LP.

Introduction

Oral lichen planus (LP) is a severe and painful form of LP, and is often resistant to topical corticosteroid therapy. Recently, some open trials demonstrated that topical tacrolimus therapy, which has been approved as a safe treatment for atopic dermatitis,[1,2] was effective for chronic erosive oral LP.[3,4] Here, we report two patients with severe recalcitrant erosive oral LP, who dramatically benefited from topical tacrolimus therapy.

Case 1

A 64-year-old man presented at our outpatient clinic with a 5-month history of painful erosions on his entire lower lip and buccal mucosa. Physical examination revealed irregular-shaped, blood-encrusted erosions with peripheral white streaks on his lower lip and buccal mucosa(fig. 1a). A biopsy specimen taken from his lower lip confirmed the diagnosis of oral LP (fig. 2a). Because he had been unsuccessfully treated with topical corticosteroids at several dermatological facilities, treatment with 0.1% topical tacrolimus, twice a day, was initiated. He experienced rapid relief from pain within a week of treatment. After 5 weeks of treatment, a dramatic improvement had been obtained on both his lips and buccal mucosa (fig. 1b). No significant irritation or recurrence was observed on continuous application during the 6-month follow-up period, and his blood tacrolimus level was kept within a safe level (2.5 ng/mL).

Case 2

A 68-year-old man developed a painful erosion on his lower right lip 2 months before his first arrival at our outpatient clinic. Physical examination revealed a 2.0×1.0 cm blood-encrusted erosion with peripheral white streaks on his right lower lip (fig. 1c). Race-form white streaks and irregular-shaped erosions were also present on his buccal mucosa. Histopathological analysis

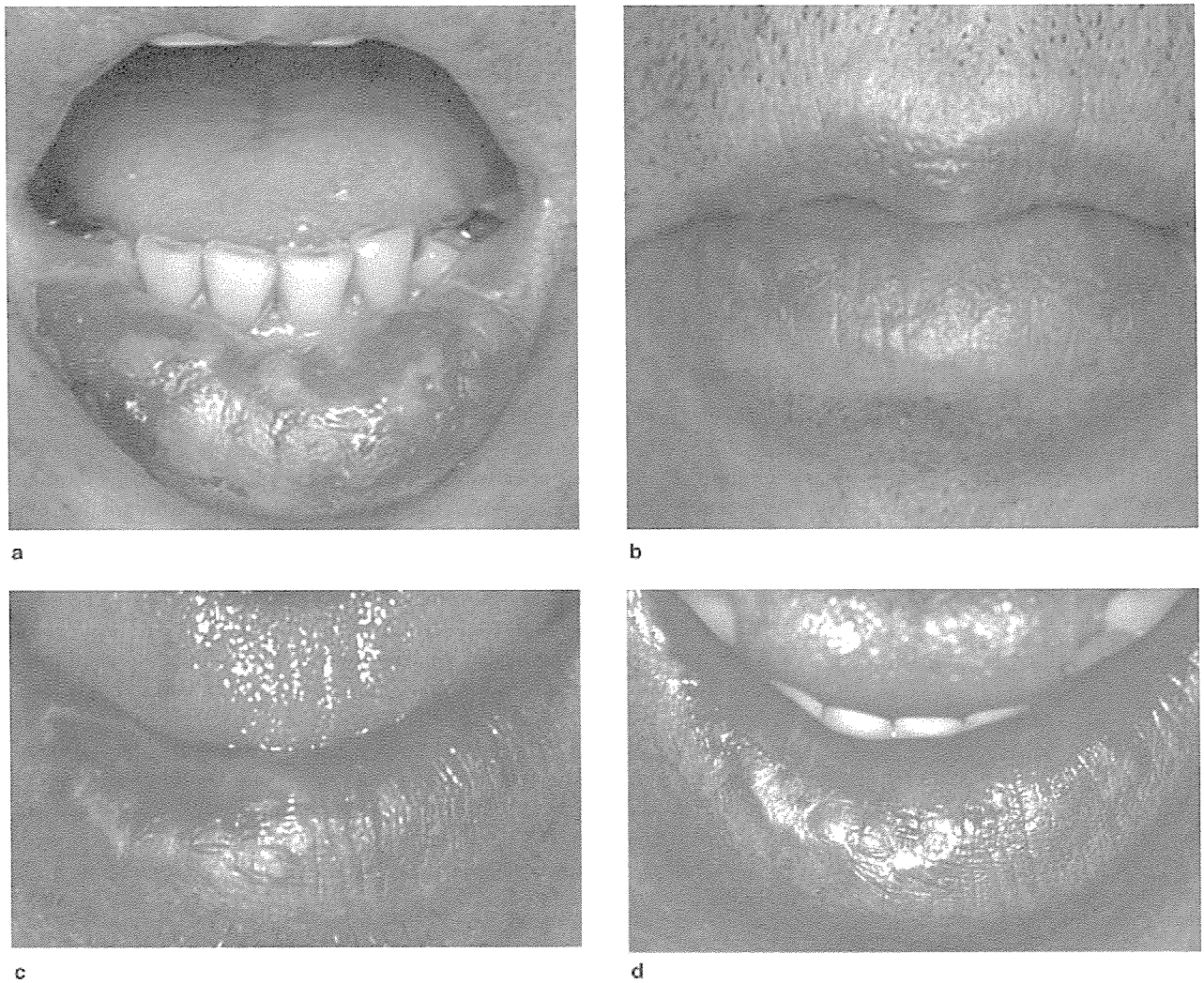

fig. 1 Clinical appearances of case 1 (a, b) and case 2 (c, d). (a) Irregular-shaped, blood-encrusted erosions with peripheral white streaks were observed on the entire lower lip. (b) After 5 weeks of treatment with topical tacrolimus, a dramatic improvement was observed. (c) A single 2.0 × 1.0 cm, blood-encrusted erosion with peripheral white streaks was present on the lower right lip. (d) A dramatic improvement was observed after 4 weeks of treatment with topical tacrolimus.

of a biopsy specimen taken from his lower lip confirmed a diagnosis of oral LP (fig. 2b). Because of his poor response to previous topical corticosteroid therapy, treatment with 0.1% topical tacrolimus, twice a day, was initiated. He experienced a rapid and dramatic improvement of both lesions within 4 weeks of treatment (fig. 1d). No significant irritation or recurrence was observed on continuous topical application of tacrolimus during the 6-month follow-up period.

Discussion

In contrast to cutaneous lesions, oral LP is often resistant to topical corticosteroid therapy.[5] Tacrolimus has powerful immunosuppressive activities by inhibiting T-cell production of proinflammatory cytokines.[6,7] Although the aetiology of LP is still unknown, cell-mediated immune reactions involving T lymphocytes are thought to play a central role. This may be one reason why topical application of tacrolimus could induce a rapid improvement in oral LP.[4] Although a minority of patients experience side-effects, such as a burning sensation and sore throat, these side-effects were not troublesome enough to discontinue topical tacrolimus application.[3] In our cases, no irritation was observed even after application onto the severely eroded lesions. There is also a concern that blood tacrolimus levels could increase during the treatment of these erosive lesions. According to previous reports, blood tacrolimus levels are not significantly different whether tacrolimus is used for oral LP or atopic dermatitis.[1,2,8] In contrast to the

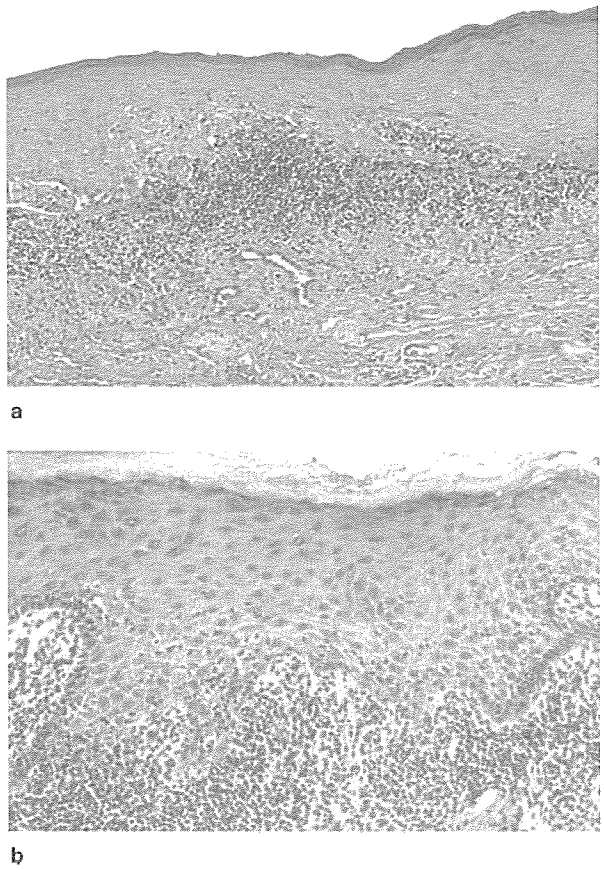

fig. 2 (a) Biopsy specimen of case 1 showing band-like infiltration of lymphocytes at the dermal–epidermal interface accompanied by vacuolar alteration of the basal keratinocyte layer and the presence of scattered necrotic keratinocytes. (b) Biopsy specimen of case 2 showing irregular acanthosis and focal hypergranulosis of the mucous epithelia accompanied by vacuolar alterations in the basal keratinocyte layer and a band-like infiltration of lymphocytes.

report by Olivier *et al.*,[4] the blood tacrolimus level in case 1 was minimally elevated (2.5 ng/mL). However, the tacrolimus level was still maintained within safe levels,[9,10] and was less than the recommended therapeutic range (5.0–20.0 ng/mL). Therefore, direct local effects may be the major contributing factors providing the therapeutic benefit observed in our case, although some systemic effects may partially have affected the clinical outcome.

Although flare-ups are commonly observed after discontinuing topical tacrolimus application,[3,4] and long-term side-effects still remain unknown, topical tacrolimus is suggested to be a well-tolerated, effective therapy for oral LP.

References

1 Morrison L, Kratochvil FJ, Gorman A. An open trial of topical tacrolimus for erosive oral lichen planus. *J Am Acad Dermatol* 2002; **47**: 617–620.

2 Ruzicka T, Bieber T, Schopf E *et al.* A short-term trial of tacrolimus ointment for atopic dermatitis. *N Engl J Med* 1997; **337**: 816–821.

3 Rozycki TW, Rogers RS III, Pittelkow MR *et al.* Topical tacrolimus in the treatment of symptomatic oral lichen planus: a series of 13 patients. *J Am Acad Dermatol* 2002; **46**: 27–34.

4 Olivier V, Lacour JP, Mousnier A *et al.* Treatment of chronic erosive oral lichen planus with low concentrations of topical tacrolimus. *Arch Dermatol* 2002; **138**: 1335–1338.

5 Vente C, Reich K, Rupprecht R, Neumann C. Erosive mucosal lichen planus: response to topical treatment with tacrolimus. *Br J Dermatol* 1999; **140**: 338–342.

6 Kelly PA, Burckart GJ, Venkataramanan R. Tacrolimus: a new immunosuppressive agent. *Am J Health Syst Pharm* 1995; **52**: 1521–1535.

7 Ruzicka T, Assmann T, Homey B. Tacrolimus: the drug for the turn of the millennium? *Arch Dermatol* 1999; **135**: 574–580.

8 Kaliakatsou F, Hodgson TA, Lewsey JD *et al.* Management of recalcitrant ulcerative oral lichen planus with topical tacrolimus. *J Am Acad Dermatol* 2002; **46**: 35–41.

9 Kershener RP, Fitzsimmons WE. Relationship of FK506 whole blood concentrations and efficacy and toxicity after liver and kidney transplantation. *Transplantation* 1996; **62**: 920–926.

10 The European FK506 Multicenter Psoriasis Study Group. Systemic tacrolimus (FK506) is effective for the treatment of psoriasis in a double-blind, placebo-controlled study. *Arch Dermatol* 1996; **132**: 419–423.

PRENATAL DIAGNOSIS
Prenat Diagn 2006; **26**: 1260–1261.
Published online in Wiley InterScience
(www.interscience.wiley.com) **DOI:** 10.1002/pd.1603

INVITED COMMENTARY: CURRENT ISSUES IN OBSTETRICS AND GENETICS

Prenatal diagnosis of epidermolysis bullosa

Hiroshi Shimizu*

Department of Dermatology, Hokkaido University Graduate School of Medicine, Sapporo, Japan

WHAT IS EPIDERMOLYSIS BULLOSA (EB)?

Epidermolysis bullosa (EB) comprises a large heterogeneous group of hereditary dermatoses characterized by skin fragility caused by gene mutations encoding a range of epidermal basement membrane molecules (Fine *et al.*, 2000). EB is categorized by the level of blister formation within the epidermal basement membrane zone, and includes the simplex type (basal keratinocyte intracellular split), junctional type (lamina lucida split) and dystrophic type (split through the uppermost dermis). EB can be further classified into ten major subtypes according to the responsible genes and the clinical phenotypes. The clinical severity and prognosis vary between each subtype from relatively minor disability to death during early infancy (Fine *et al.*, 2000).

WHICH EB SUBTYPES ARE SUITABLE FOR PND?

There are three clinically severe subtypes of EB: Hallopeau-Siemens recessive dystrophic EB (HSRD-EB), Herlitz junctional EB (HJ-EB) and junctional EB associated with congenital pyloric atresia (JEB-PA). These three subtypes are internationally recognized as the indications for prenatal diagnosis (PND) (Shimizu and Suzumori, 1999).

HSRD-EB is associated with high morbidity due to widespread skin ulcers, fusion of fingers and toes, and premature mortality due to aggressive early onset of squamous cell carcinoma. HSRD-EB is caused by mutations in *COL7A1* gene, which encodes type VII collagen, the major component of anchoring fibrils linking the epidermis to the underlying dermis.

HJ-EB, characterized by extensive non-healing ulcers and poor prognosis, is caused by mutations in one of the following genes LAMA3, LAMB3 or the LAMC2 encoding the three chains of laminin 332 (formerly known as laminin 5), which encode the α 3, β 3 and γ 2 chains. The majority of HJ-EB patients die within one year after birth.

JEB-PA is caused by mutations in INTGA6 or INTGB4 encoding α 6 or β 4 integrin located in the epidermal basement membrane. JEB-PA demonstrates both severe skin ulcers and congenital pyloric atresia with a poor general prognosis (Sawamura *et al.*, 2003).

FROM FETAL SKIN BIOPSY TO DNA-BASED PND

In the 1980s, PND for EB was started using the fetal skin biopsy technique. Initially, the diagnosis was based on the ultrastructural plane of cleavage and on particular morphological abnormalities of the hemidesmosome and anchoring fibrils using transmission electron microscopy. Subsequently, with the generation of reliable monoclonal antibodies specific to epidermal basement membrane molecules, immunohistochemistry was performed on fetal skin. In the 1990s, the genes responsible for respective EB subtypes and the family-specific mutations were identified. This led to the feasibility of DNA-based PND using fetal DNA extracted from chorionic villi or amniotic cells. The majority of DNA-based PND have been performed either by direct assessment of previously identified pathogenic mutations or by using indirect linkage markers (Shimizu and Suzumori, 1999).

While the majority of PND for EB are currently based on analyzing the fetal DNA, identification of specific mutations in the causative gene cannot be achieved in all EB cases. Therefore, the fetal skin biopsy technique is still used for PND in these specific cases, though the number is now limited.

PRE-IMPLANTATION GENETIC DIAGNOSIS (PGD) FOR EB

Analysis of fetal skin biopsies and DNA-based PND, however, allows for fetal diagnosis only after pregnancy has been established. Pre-implantation genetic diagnosis (PGD) involves a single cell biopsy from the six-to-ten cell blastomere stage of the fertilized embryo followed by DNA mutational analysis (Handyside *et al.*, 1990). Disease-free embryos are then implanted into the uterus, thereby avoiding any pregnancy termination procedures usually associated with conventional PND methods. Since its initial clinical application in 1990,

*Correspondence to: Hiroshi Shimizu, Department of Dermatology, Hokkaido University Graduate School of Medicine, Sapporo, Japan. E-mail: shimizu@med.hokudai.ac.jp

Received: 26 September 2006
Accepted: 5 October 2006

PGD has become a well-established option (Handyside *et al.*, 1990).

In contrast to the large number of DNA-based PND for EB, however, only a few cases of PGD have been described. Two cases of PGD for HJ-EB have been reported; although only a biochemical pregnancy that failed to come to full term was achieved in each case (Cserhalmi-Friedman *et al.*, 2000). In 2006, the first successful outcome of a healthy baby by PGD of EB was reported (Fassihia *et al.*, 2006). In that case, single cell PCR amplification of the microsatellites flanking the *COL7A1* gene was used for PGD of HSRD-EB. This research group also reported a successful PGD for another genodermatosis, skin fragility-ectodermal dysplasia syndrome; in this case, the baby was born healthy (Fassihi *et al.*, 2006). PGD provides additional options for couples at risk of severe EB who are determined to avoid termination of the pregnancy. However, PGD is practiced at few centers worldwide. Moreover, several countries, including Japan, take a careful, ethical approach to PGD, and only specific diseases and conditions are approved as indication of PGD.

FUTURE PERSPECTIVES FOR PND OF EB

The most important clinical, ethical and practical issue for PND of EB is what we can do when the fetus is diagnosed as being affected. In autosomal recessive disorders such as severe EB, there is a 25% probability of the fetus being affected if the parents are heterozygous carriers of the genetic mutation. Recently, various experimental treatments of EB have been reported, including those targeting the deficient genes or proteins (Chen *et al.*, 2002; Woodley *et al.*, 2004; Goto *et al.*, 2006a, 2006b).

Related to this, we have developed a mouse model of junctional EB that can survive and be utilized in therapeutic experiments of EB (Nishie *et al.*, 2006). The EB phenotype of its mouse model was completely eliminated by introducing the corresponding human gene, indicating that gene therapy for EB patients and possibly fetuses might be effective. If the treatment of an affected fetus with EB becomes feasible in the future, the clinical importance of PND will also increase.

REFERENCES

Chen M, Kasahara N, Keene DR, *et al.* 2002. Restoration of type VII collagen expression and function in dystrophic epidermolysis bullosa. *Nat Genet* **32**: 670–675.

Cserhalmi-Friedman PB, Tang Y, Adler A, Krey L, Grifo JA, Christiano AM. 2000. Preimplantation genetic diagnosis in two families at risk for recurrence of Herlitz junctional epidermolysis bullosa. *Exp Dermatol* **9**: 290–297.

Fassihia H, Renwickb PJ, Blackb C, McGrath JA. 2006. Single cell PCR amplification of microsatellites flanking the COL7A1 gene and suitability for preimplantation genetic diagnosis of Hallopeau-Siemens recessive dystrophic epidermolysis bullosa. *J Dermatol Sci* **42**: 241–248.

Fassihi H, Grace J, Lashwood A, *et al.* 2006. Preimplantation genetic diagnosis of skin fragility–ectodermal dysplasia syndrome. *Br J Dermatol* **154**: 546–550.

Fine JD, Eady RA, Bauer EA, *et al.* 2000. Revised classification system for inherited epidermolysis bullosa: report of the second International consensus meeting on diagnosis and classification of epidermolysis bullosa. *J Am Acad Dermatol* **42**: 1051–1066.

Goto M, Sawamura D, Ito K, *et al.* 2006a. Fibroblasts show more potential as target cells than keratinocytes in COL7A1 gene therapy of dystrophic epidermolysis bullosa. *J Invest Dermatol* **126**: 766–772.

Goto M, Sawamura D, Nishie W, *et al.* 2006b. Targeted Skipping of a single exon harboring a premature termination codon mutation: implications and potential for gene correction therapy for selective dystrophic epidermolysis bullosa patients. *J Invest Dermatol* in press.

Nishie W, Sawamura D, Goto M, *et al.* 2006. Humanization of autoantigen. *Nat Med* (in press).

Handyside AH, Kontogianni EH, Hardy K, Winston RML. 1990. Pregnancies from biopsied human preimplantation embryos sexed by Y-specific DNA amplification. *Nature* **344**: 768–770.

Sawamura D, McMillan JR, Akiyama M, Shimizu H. 2003. Epidermolysis bullosa: directions for future research and new challenges for treatment. *Arch Dermatol Res* **295**(Suppl. 1): S34–S42.

Shimizu H, Suzumori K. 1999. Prenatal diagnosis as a test for genodermatoses: its past, present and future. *J Dermatol Sci* **19**: 1–8.

Woodley DT, Keene DR, Atha T, *et al.* 2004. Injection of recombinant human type VII collagen restores collagen function in dystrophic epidermolysis bullosa. *Nat Med* **10**: 693–695.

The Invited Commentary aims to comment on topical issues in *Prenatal Diagnosis* which are of relevance to both obstetricians and medical geneticists. These commentaries are invited and each represents a personal critical analysis of the current studies of a particular subject, putting the latest research into the context of earlier work and providing implications for clinical practice.

Prenat Diagn 2006; **26**: 1260–1261.
DOI: 10.1002/pd

American Journal of Pathology, Vol. 168, No. 1, January 2006

DOI: 10.2353/ajpath.2006.050469

Epithelial and Mesenchymal Cell Biology

Expression of RNA-Binding Protein Musashi in Hair Follicle Development and Hair Cycle Progression

Yoriko Sugiyama-Nakagiri,* Masashi Akiyama,* Shinsuke Shibata,† Hideyuki Okano,† and Hiroshi Shimizu*

From the Department of Dermatology, Hokkaido University Graduate School of Medicine, Sapporo; and the Department of Physiology,† Keio University School of Medicine, Tokyo, Japan*

Epithelial stem cells reside in the hair follicle (HF) bulge region and possess the ability to differentiate into a variety of cutaneous epithelial cells. The evolutionarily conserved Musashi family of RNA-binding proteins is associated with maintenance and/or asymmetric cell division of neural progenitor cells, and a mammalian Musashi protein is expressed in various epithelial stem/progenitor cells, including gut, stomach, and mammary gland. Thus, we hypothesized that Musashi might be expressed in stem cells and early progenitor cells of HF epithelium. Reverse transcriptase-polymerase chain reaction and immunoblotting identified Musashi-1 (Msi-1) and Musashi-2 (Msi-2) mRNA and protein in cultured mouse keratinocytes, but only Msi-1 was identified in human keratinocytes. In mice, immunohistochemical studies showed that Msi-1 and Msi-2 were expressed in the epidermis and HFs from E14.5 until adulthood. In the early anagen phase, Msi-1 and Msi-2 were expressed in the bulge and secondary germ cells and subsequently in inner root sheath (IRS) cells, especially the middle IRS cells, during the late anagen phase. In human skin, Msi-1 was detected in fetal HF cells but not in adult HFs. These observations suggest that Musashi functions not only in the asymmetric division of early progenitor cells but also in the differentiation of IRS cells during HF development and hair cycle progression. ***(Am J Pathol 2006, 168:80–92; DOI: 10.2353/ajpath.2006.050469)***

During skin development, a population of multipotent stem cells gives rise to both the epidermis and its appendages, including hair follicles (HFs). HF morphogenesis is triggered by a series of epithelial-mesenchymal cues, and recent findings obtained from mutant mice have revealed various signaling molecules involved in HF development and hair cycle progression.[1] Other studies have reported that HF stem cells lie in the bulge region of HFs.[2–5] Cells in this region have a high colony-forming capacity,[6,7] are slow cycling, and have a quiescent nature.[8] Transplantation studies suggest that these bulge cells possess the ability to differentiate into multiple different types of cutaneous epithelial cells, including the sebaceous gland and even epidermal cells.[8–12] Some putative HF stem cell markers have been reported, but none of them have been proven to be definitive markers.

The Musashi family of proteins is an evolutionarily conserved group of RNA-binding proteins, initially identified in *Drosophila* where they are required for early asymmetric cell divisions in the sensory organ precursor cells.[13–15] In mammals, Msi-1 and Msi-2 have been identified in mice,[14,16] but only Msi-1 is expressed in humans.[17] It has subsequently been demonstrated that Msi-1 and Msi-2 are selectively expressed in neural progenitor cells, including stem cells, and have key roles in the maintenance of the stem cell state and differentiation.[14–16,18–20] Moreover, Msi-1 has been shown to be a positive regulator of Notch-signaling through its interaction with m-Numb mRNA.[21] Outside the nervous system, Msi-1 is a selective marker for various epithelial stem or early progenitor cells present in intestine,[22–24] gastric mucosa,[25] and mammary gland,[26] among others. Because similar asymmetric divisions are thought to maintain the HF stem cell compartment, we hypothesized that Musashi might be expressed in either HF stem cells or early progenitor cells.

In this report, we have examined the expression pattern of Musashi family proteins during HF development and adult hair cycles in both mice and humans. We found that Msi-1 and Msi-2 were expressed in mouse stem cells

Supported in part by a grant-in-aid from the Ministry of Education, Science, Sports, and Culture of Japan (Kiban B 16390312 to M.A.) and by a Health and Labor Sciences research grant from the Ministry of Health, Labor, and Welfare of Japan (H16-Research on Measures for Intractable Diseases-05 to H.S.).

Accepted for publication September 13, 2005.

Address reprint requests to Masashi Akiyama, M.D., Ph.D., Department of Dermatology, Hokkaido University Graduate School of Medicine, N15 W7, Sapporo 060-8638, Japan. E-mail: akiyama@med.hokudai.ac.jp.

in the bulge region. In addition, Msi-1/2 was also expressed in the secondary hair germ, the HF matrix, and the inner root sheath (IRS) cells, at all developmental stages until adulthood. In humans, Msi-1 expression sites were similar to those in mice, although Msi-1 was expressed only in developing skin. These observations suggest that Musashi functions not only in asymmetric stem cell or early progenitor cell division but also in the differentiation of IRS cells during HF development and hair cycle progression.

Materials and Methods

Cell Culture

Neonatal human keratinocytes (NHKs) were purchased from Cambrex Bio Science Walkersville, MD. Mouse keratinocytes were obtained from C57BL/6J mouse skin after 3 to 5 hours of dispase enzyme digestion, followed by trypsinization of the separated epidermis. Both human and mouse keratinocyte cells were cultured in defined keratinocyte serum-free medium (Invitrogen, San Diego, CA). Both human and mouse keratinocytes were cultured in low Ca^{2+} conditions (0.09 mmol/L) to maintain a basal cell-like population of undifferentiated cells. To induce terminal differentiation, $CaCl_2$ was added directly to the culture media at a final concentration of 2 mmol/L. Photographs were taken using a Nikon Coolpix (Nikon, Tokyo, Japan).

Semiquantitative Reverse Transcriptase-Polymerase Chain Reaction (RT-PCR)

Total RNA was extracted using RNeasy (Qiagen, Chatsworth, CA). cDNA was synthesized by reverse transcription of 1 μg of total RNA, using a cDNA synthesis kit (Invitrogen). The following sets of oligonucleotide primers were used: for mouse Msi-1, 5′-CGAGCTCGACTCCAAAACAAT-3′ (sense) and 5′-GGCTTTCTTGCATTCCACCA-3′ (anti-sense); mouse Msi-2, 5′-GTCTGCGAACACAGTAGTGGAA-3′ (sense) and 5′-GTAGCCTCTGCCATAGGTTGC-3′ (anti-sense); human Msi-1, 5′-GGCTTCGTCACTTTCATGGACCAGGCG-3′ (sense) and 5′-GGGAACTGGTAGGTGTAA-3′ (anti-sense); human keratin 1, 5′-CACTTATTCCGGAGTAACCAG-3′ (sense) and 5′-GAATAGGATGAGCTAGTGTAA-3′ (anti-sense); mouse glyceraldehyde-3 phosphate-dehydrogenase (mGAPDH), 5′-TTAGCCCCCCTGGCCAAGG-3′ (sense) and 5′-CTTACTCCTTGGAGGCCATG-3′ (anti-sense); human GAPDH (hGAPDH), 5′-TCATCTCTGCCCCCTCTGCT-3′ (sense) and 5′-CGACGCCTGCTTCACCACCT-3′ (anti-sense). The PCR amplification for Musashi was performed as follows: 95°C for 10 minutes, 40 cycles of 94°C for 30 seconds, 55°C for 30 seconds, and 72°C for 1 minute, with a final extension step of 72°C for 5 minutes. Keratin 1 and GAPDH were amplified for 25 cycles. PCR products were analyzed by agarose gel electrophoresis.

Immunoblotting

Cell lysates were prepared by homogenization in lysis buffer (50 mmol/L Tris-HCl, pH 7.6, 150 mmol/L NaCl, 1% Nonidet P-40, 0.1% sodium dodecyl sulfate, 0.25% sodium deoxycholate), followed by centrifugation at 15,000 rpm for 5 minutes. Cell lysates (100 μg of protein per lane) were resolved on 12.5% sodium dodecyl sulfate-polyacrylamide gel electrophoresis gels that were then electroblotted onto Immobilon-P membranes (Millipore, Bedford, MA) using a wet transfer apparatus. Membranes were probed with either rat monoclonal anti-Msi-1 antibody (final dilution, 1:500)[18] or rabbit polyclonal anti-Msi-2 (final dilution, 1:500)[16] antiserum. Proteins were detected with horseradish peroxidase-conjugated secondary antibodies (Jackson Immunoresearch Laboratory, West Grove, PA), and specific bands were visualized by chemiluminescence.

Mice and Tissue Preparation

C57BL/6J mice were purchased from Clea Japan Inc. (Tokyo, Japan). The mice were kept in isolator cages in a barrier facility under a 12-hour light cycle and maintained under specific pathogen-free conditions. Pregnant mice were purchased to get embryos at 14 to 18 days of gestation.

For hair morphogenetic studies, the dorsal skin samples were obtained from untreated newborn mice (male and female) on days 1, 4, 8, 11, 18, and 21 after birth. The samples were processed for immunohistological staining. For hair cycle experiments, 7-week-old female C57BL/6J mice were purchased. After conditioning for 1 week, the anagen phase of the hair growth cycle was induced by gently depilating their dorsal hair shafts using depilatory chemicals. They were sacrificed at 0, 1, 4, and 11 days after depilation for further studies of Msi-1 expression at specific stages of the hair cycle, ie, the anagen phase (1, 4, and 11 days after depilation) and the telogen phase (0 days after depilation).

Human Fetal and Adult Skin Specimens

Human embryonic and fetal skin specimens were obtained from abortuses of 49 to 163 days estimated gestational age (EGA) through the Central Laboratory of Human Embryology at the University of Washington, Seattle, WA, with the approval of the Human Subjects Review Board and in accordance with the United States Department of Health, Education, and Welfare policies. The ages, the autopsy sites, and the numbers of embryos or fetuses included in this study were as follows: 49 to 64 days EGA, scalp (n = 2), trunk (n = 2); 65 to 84 days EGA, scalp (n = 3), trunk (n = 2); 85 to 104 days EGA, scalp (n = 2), trunk (n = 2); 105 to 135 days EGA, scalp (n = 2), trunk (n = 2); and >135 days EGA, scalp (n = 2), trunk (n = 2). Two or three skin specimens from each fetus were used for this study. EGA was determined from maternal histories, fetal measurements (crown-rump and foot length), and

comparative histological appearance of the epidermis. Normal adult human skin samples were obtained at skin surgical operations of benign subcutaneous tumors under fully informed consent at Department of Dermatology, Hokkaido University School of Medicine.

Detection of Slow-Cycling Cells

To examine the proliferating ability of the skin cells, we labeled neonatal C57BL/6J mice skin with subcutaneous injections of 5-bromo-2-deoxyuridine (BrdU; 50 μg/g body weight) from day 3 of life, twice a day for 3 days. The mice were sacrificed, and skin samples were obtained for further immunolabeling immediately after the BrdU labeling until 2 weeks after the start of the initial labeling to demonstrate the entire labeled cell population and label-retaining cells (slow-cycling cells), respectively. We performed double immunostaining for BrdU and Msi-1 or Msi-2 using the following methods to demonstrate the proliferating cells or label retaining cells and Msi-positive cells in the same tissue sections.

Immunofluorescent Labeling

The dorsal skin samples removed from the mice were immediately frozen in OCT compound (Tissue-Tek; Sakura Finetechnical, Tokyo, Japan) and cut at a thickness of 6 μm. Sections were fixed with 4% paraformaldehyde for 15 minutes at 4°C. The sections were then placed in 0.01 mol/L citrate buffer, pH 6.0, and microwave-treated (500 W) for 10 minutes to facilitate antigen retrieval. Sections were incubated with 10% goat serum in PBS for 1 hour and then incubated with primary antibodies at 4°C overnight: anti-mouse Msi-1 antibody[18] (14H-1; final dilution, 1:1000), anti-mouse Msi-2 antibody[16] (final dilution, 1:100), anti-BrdU antibody (Roche, Mannheim, Germany; final dilution, 1:100), anti-CD34 antibody (BD Pharmingen, San Diego, CA; final dilution, 1:50), or anti-Ki67 antibody (Novocastra, Newcastle on Tyne, UK; final dilution, 1:250). The sections were incubated with secondary antibodies at room temperature for 1 hour: fluorescein isothiocyanate (FITC)-conjugated anti-rat IgG (Jackson Immunoresearch Laboratory; final dilution, 1:50), FITC-conjugated anti-rabbit-IgG (Jackson Immunoresearch Laboratory; final dilution, 1:50), FITC-conjugated anti-mouse-IgG (Jackson Immunoresearch Laboratory; final dilution, 1:50), or tetramethyl-rhodamine isothiocyanate anti-mouse IgG (Southern Biotechnology Associates, Inc., Birmingham, AL; final dilution, 1:50). The sections were then incubated with 10 μg/ml of propidium iodide at 37°C for 10 minutes for nuclear counterstaining. Sections were observed under an Olympus Fluoview confocal laser-scanning microscope (Olympus, Tokyo, Japan).

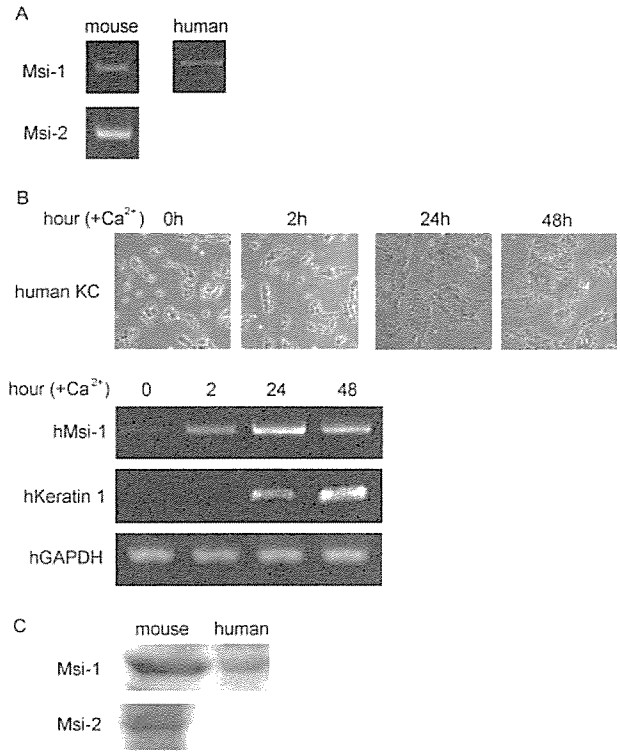

Figure 1. Msi-1 and Msi-2 expression in mouse and human keratinocytes. The expression of Msi-1 and Msi-2 was detected in mouse and human keratinocytes. **A:** RT-PCR analysis of Msi-1 and Msi-2 mRNA expression in mouse and human keratinocytes cultured in low Ca^{2+} medium (0.09 mmol/L). Expression of mouse Msi-1, Msi-2 (Msi-1 and Msi-2, **left**), and human Msi-1 (Msi-1, **right**) was detected in cultured keratinocytes. **B:** Normal human keratinocytes (NHKs) cultured in low Ca^{2+} medium remain undifferentiated, and raising the Ca^{2+} concentration greater than 2 mmol/L induces the expression of the differentiation-associated molecule keratin 1 and morphological changes including stratification. Msi-1 expression increased 2 hours after raising Ca^{2+} culture levels for human keratinocytes. GAPDH expression is shown as an internal control. **Top**: Human Msi-1 expression (hMsi-1); **middle**: human keratin-1 expression (hKeratin 1); **bottom**: human GAPDH expression (hGAPDH). **C:** Western blot analysis of Msi-1 and Msi-2 proteins in mouse and human keratinocytes. Msi-1 was expressed in mouse and human keratinocytes (37- to 40-kd bands) and Msi-2 was detected in mouse keratinocytes (35- to 37-kd band).

Results

Expression of Msi-1 and Msi-2 mRNAs in Mouse and Human Keratinocytes

The RT-PCR-amplified products obtained using Msi-1-specific and Msi-2-specific primers showed clear bands of the predicted sizes. Msi-1 and Msi-2 gene expression was identified in mouse keratinocytes derived from C57BL/6J mice cultured in low Ca^{2+} medium (0.09 mmol/L), and Msi-1 gene expression was observed in normal human keratinocytes (NHKs) cultured in low Ca^{2+} medium (0.09 mmol/L) (Figure 1A). Msi-2 was not identified in human tissues. Thus, using human tissues, we could study only Msi-1 expression. Keratinocytes cultured in low Ca^{2+} medium (0.09 mmol/L) remain undifferentiated; raising the Ca^{2+} concentration greater than 2 mmol/L induced expression of differentiation-associated molecules and several morphological changes (Figure 1B). We found that human Msi-1 message levels increased 2 hours after

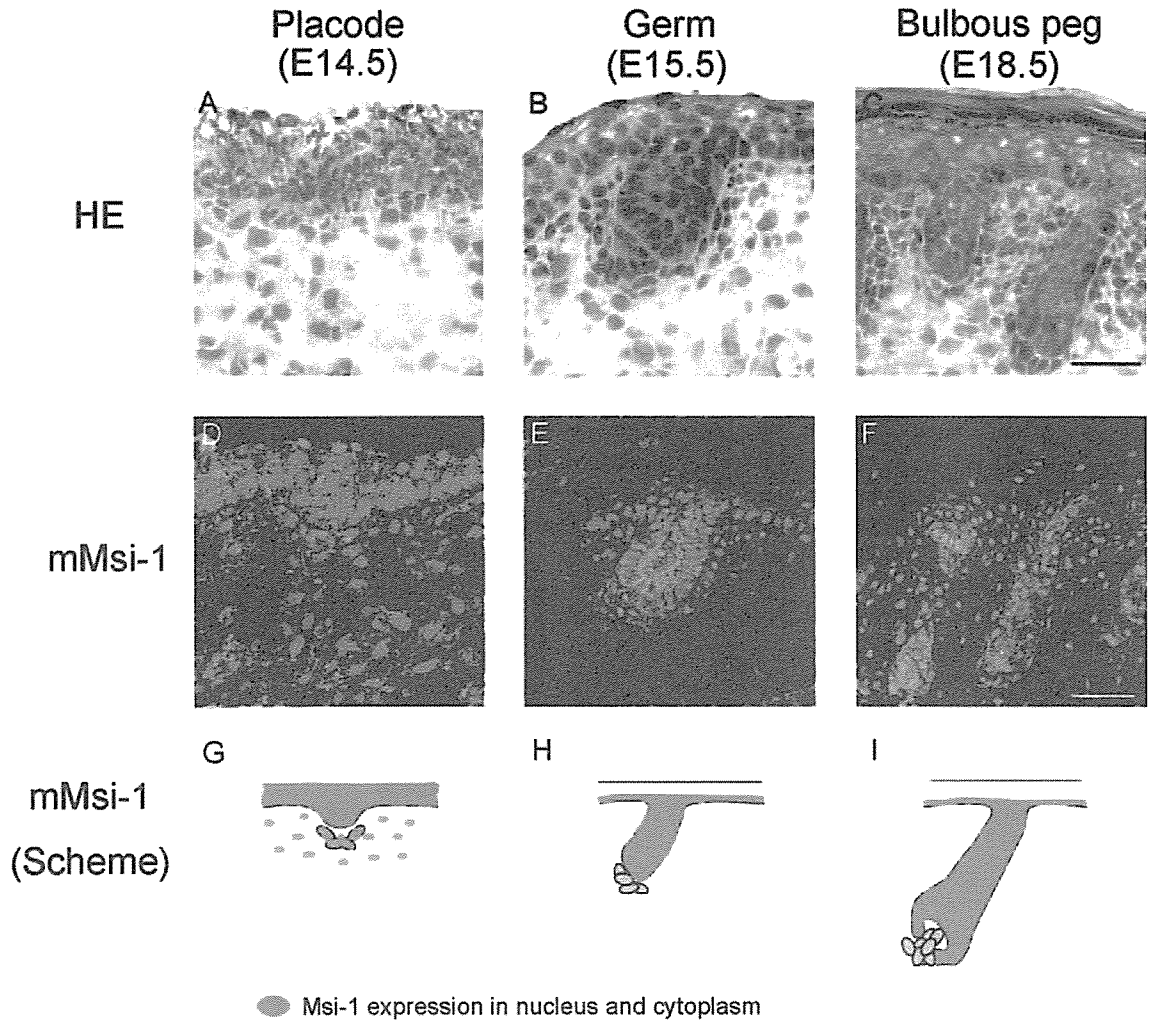

Figure 2. Msi-1 was expressed in mice embryonic skin. C57BL/6 mouse back skin samples, at the following developmental stages (E14.5, E15.5, and E18.5), were processed for immunohistological analysis of Msi-1. Sections were subjected to H&E staining (**A–C**) or immunofluorescence staining with the anti-Msi-1 antibody (**D–F**). **D–F** are confocal images in which Msi-1 fluorescence (green, FITC) and nuclear stain (red, propidium iodide) were merged. Msi-1 was expressed in the undifferentiated epidermis and in the dermal cells at E14.5. Msi-1 was expressed in hair germ and bulbous hair peg at each developmental stage. **G–I:** Schematic representation of immunoreactivity patterns of Msi-1 during murine embryonic epidermal development. Green shows Msi-1 expression in both the nucleus and cytoplasm. **A**, **D**, and **G**, at E14.5; **B**, **E**, and **H**, at E15.5; **C**, **F**, and **I**, at E18.5. Scale bars, 50 μm.

raising the extracellular calcium concentration to 2 mmol/L, while the GAPDH message expression levels were unaffected (Figure 1B). In immunoblots of mouse and human cultured keratinocytes, the anti-Msi-1 and anti-Msi-2 antibodies recognized the expected protein bands (Figure 1C). Msi-1 was detected as a major band of 37 to 40 kd in the human and mouse keratinocyte extracts, and Msi-2 was detected as a major band of 35 to 37 kd in the mouse keratinocyte extract.

Expression of Msi-1 Protein during Hair Morphogenesis in Mouse Skin

At E14.5, weak Msi-1 expression was observed throughout the entire, as yet, unkeratinized epidermis and the hair placode (Figure 2, A, D, and G). In addition, Msi-1 was expressed in the dermal cells surrounding the hair placode and in the upper dermis. At E15.5, the inner cells of the hair germ showed strong expression of Msi-1 protein compared with the outermost cells of the hair germ and the dermal cells (Figure 2, B, E, and H). At E18.5, Msi-1 was highly expressed throughout the entire bulbous hair peg and interfollicular epidermal basal layer (Figure 2, C, F, and I).

Msi-1 Is Expressed in the Restricted Areas of the HF IRS during the First Hair Cycle (Neogenesis) in Neonatal Mice

During the anagen phase of HF neogenesis in 1-day-old mice, Msi-1 was expressed throughout the entire developing HF and within the basal cells of the interfollicular epidermis (Figure 3, A and G). This expression pattern was similar to that in E18.5 skin (Figure 2, F and I). In 4-day-old mice, during the anagen phase, Msi-1-positive cells were seen in the outermost layer of IRS cells in the middle of the HF, just below the IRS start of keratinization

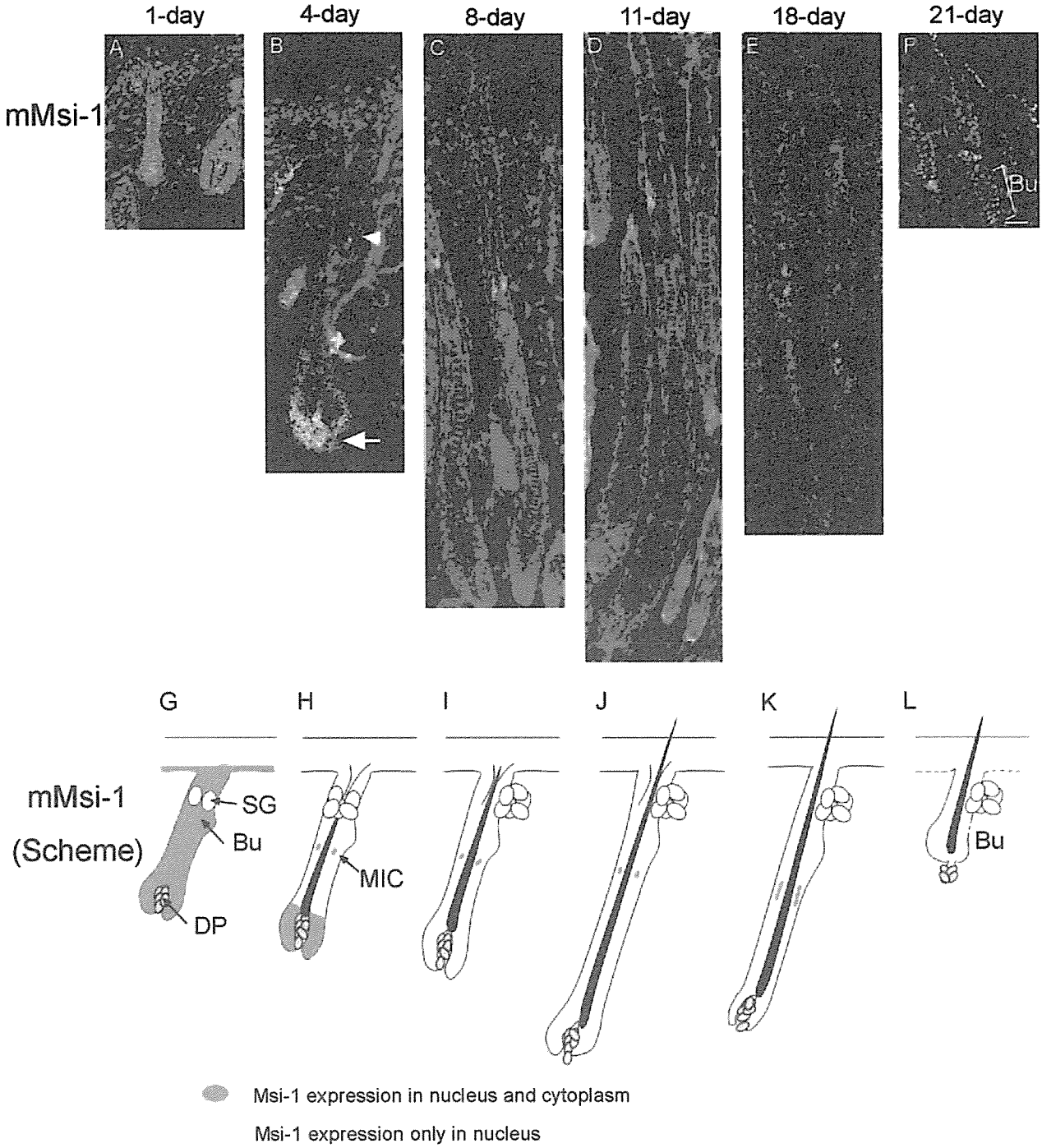

Figure 3. Msi-1 expression in mouse neonatal skin. Dorsal skin samples from C57BL/6 newborn mice on days 1, 4, 8, 11, 18, and 21 after birth were examined. Msi-1 was expressed in matrix and middle IRS cells (MICs) at an early anagen phase, and at late anagen to early catagen phases Msi-1 was found only in MICs. At the transition from telogen to early anagen phase, Msi-1 was expressed in bulge cells. **A** and **G:** One-day-old (anagen); **B** and **H:** 4-day-old (anagen); **C** and **I:** 8-day-old (anagen); **D** and **J:** 11-day-old (anagen); **E** and **K:** 18-day-old (early catagen); **F** and **L:** 21-day-old (during the transition from telogen to anagen state) mice. **G–L:** Schematic representation of Msi-1 immunoreactivity patterns during murine neonatal skin. Green shows Msi-1 expression in nucleus and cytoplasm. Yellow shows Msi-1 expression only in nucleus. SG, sebaceous gland; Bu, bulge; DP, dermal papilla; MIC, middle IRS cells. Scale bar, 50 μm.

(Figure 3, B (arrowhead) and H). We tentatively termed these cells "middle IRS cells" (MICs). The HF matrix cells were also Msi-1-positive (Figure 3, B (arrow) and H). From the age of 8 days (11 and 18 days old), during the late anagen to early catagen phase, only MICs showed strong Msi-1 immunoreactivity (Figure 3, C–E and I–K). These MICs expressed Msi-1 both in the cytoplasm and in the nucleus. The number of Msi-1-positive MICs in the early catagen HF was greater than those in the anagen HF (Figure 3, E and K). Outer root sheath cells were completely devoid of Msi-1 expression throughout the anagen to catagen phase during the first hair cycle.

Msi-1-positive MICs disappeared during the transition phase, telogen to early anagen, at 21 days (Figure 3, F and L). At this stage, Msi-1 was expressed in the nucleus of the bulge, the secondary germ, and the epidermal cells.

Msi-1 Is Expressed in the Bulge and Secondary Hair Germ Cells during Early Anagen and in the MIC and Matrix Cells during the Late Anagen Phase in Adult Mice

In the depilation-induced adult hair cycle, at day 0 immediately after depilation, in the telogen phase, Msi-1-positive cells were not seen in the HF, although Msi-1 was expressed in the interfollicular epidermal basal cell nuclei (Figure 4, A, D, and J). During the early steps of telogen-anagen transition, at days 1 to 4 after depilation, Msi-1 was expressed in the bulge region and secondary germ cells (Figure 4, B, C, E, F, K, L). At that time, the bulge cells expressed CD34, a putative HF stem cell marker[10–12] (Figure 4G), and Msi-1-positive cells were also positive for the proliferation marker Ki67 antigen (Figure 4H). During the late anagen phase, 11 days after depilation, MICs were Msi-1-positive, similar to the Msi-1-positive MICs seen during the anagen phase of HF development (Figure 4, I and M). In addition, the anagen HF expressed Msi-1 protein in the hair matrix cells (Figure 4, I and M). In these cells, Msi-1 was expressed both in the cytoplasm and in the nuclei. Throughout the depilation induced adult hair cycle, we found Msi-1-positive nuclei in the interfollicular epidermal basal cells (Figure 4, D–F and I–M).

Msi-2 Is Expressed throughout the Entire Hair Germ, the Progenitor Cells of the IRS (preIRS) in the Developing HF, and the Entire HF IRS from the Neonatal Until Adult Stages of the Hair Cycle in Mice

We next observed the distribution of Msi-2 protein, another member of the Musashi RNA-binding protein family. We failed to find Msi-2 expression in E14.5 mouse skin (Figure 5, A, D, and G). However, at E15.5, Msi-2 was expressed throughout the entire hair germ and in the superficial layers of the epidermis (Figure 5, B, E, and H). In E18.5 and 1-day-old neonatal mouse skin, Msi-2 was expressed in the IRS cone cells, the progenitor cells for the IRS (preIRS) (Figure 5, C, F, and I; Figure 6, A and G). After birth, at 4 days and later (8, 11, and 18 days), Msi-2 was expressed in the IRS layer cells including the Msi-1-positive MICs (Figure 6, B–E and H–K). At 21-days, Msi-2 was expressed in the inner bulge region cells (Figure 6, F and L). Throughout the neonatal hair cycle, Msi-2 was expressed in the superficial layers of the epidermis (Figure 6, A–L). Similar to Msi-1, however, Msi-2 was not seen in the HF during the telogen phase (Figure 7, A, D, and H). In the mouse adult hair cycle, Msi-2 was expressed in the bulge, to a lesser extent in hair germ cells during the early anagen phase (Figure 7, B, E, I, C, F, and J), and in the IRS layer cells including MICs during the late anagen stage (Figure 7, G and K).

Expression of Msi-1 Is Seen in the Developing Human HF but Not in the Adult Human HF

During the early human HF morphogenesis (65 to 84 days EGA), Msi-1 protein was expressed throughout the entire hair germ, in the cells forming dermal cell condensation, and in the basal layer of the interfollicular epidermis (Figure 8, A and F). During the early hair peg to bulbous hair peg transition (85 to 134 days EGA), Msi-1 was expressed throughout the entire hair peg and bulbous hair peg cells and in dermal cells surrounding the hair peg and bulbous hair peg (Figure 8, B, C, G, and H). The outermost cells of the hair peg and bulbous hair peg only weakly expressed Msi-1 compared with the inner cells. In lanugo HFs (>135 days EGA), Msi-1 expression was seen in the IRS and matrix (Figure 8, E and I). We failed to find any signal in the bulge region (Figure 8, D and I). We could also not detect Msi-1 in any part of the adult HFs; however, we detected Msi-1 mRNA in NHK derived from human adult skin (data not shown).

Musashi-Positive MICs Are Distinct from Slow-Cycling Cells in the HF of Neonatal Mice

Double-immunofluorescence labeling for BrdU and Msi-1 or Msi-2 indicated that most HF epithelial cells and interfollicular epidermal keratinocytes, including MICs, were positive for BrdU just after the labeling (Figure 9, A and C). After the 2-week chase experiment, the Msi-1- or Msi-2-positive MICs failed to show significant BrdU labeling (Figure 9, B and D; arrowheads), indicating that the Musashi-positive MICs were not slow-cycling.

Discussion

The Musashi family of genes encodes RNA-binding proteins that are associated with asymmetric division and/or maintenance of neural progenitor cells.[14–16,18] Msi-1 and Msi-2 are selectively expressed in neural progenitor cells, including putative stem cells, where they have key roles in the maintenance of the stem cell state and differentiation. Furthermore, the mammalian Musashi protein is also expressed in various epithelial stem/progenitor cells, including gut, stomach, and mammary gland.[22–26] Therefore, we examined whether Musashi family proteins might be expressed in the HF bulge region, which is the niche thought to harbor the HF epithelial stem cell population.[9]

In the present study, we have demonstrated for the first time that the Musashi family proteins are expressed in the epidermis and the HF of both mouse and human skin. In mice, Msi-1 and Msi-2 mRNA and proteins were expressed in cultured keratinocytes. Furthermore, immunohistochemical studies showed that Msi-1 and Msi-2 were expressed in the epidermis and HF from the earliest

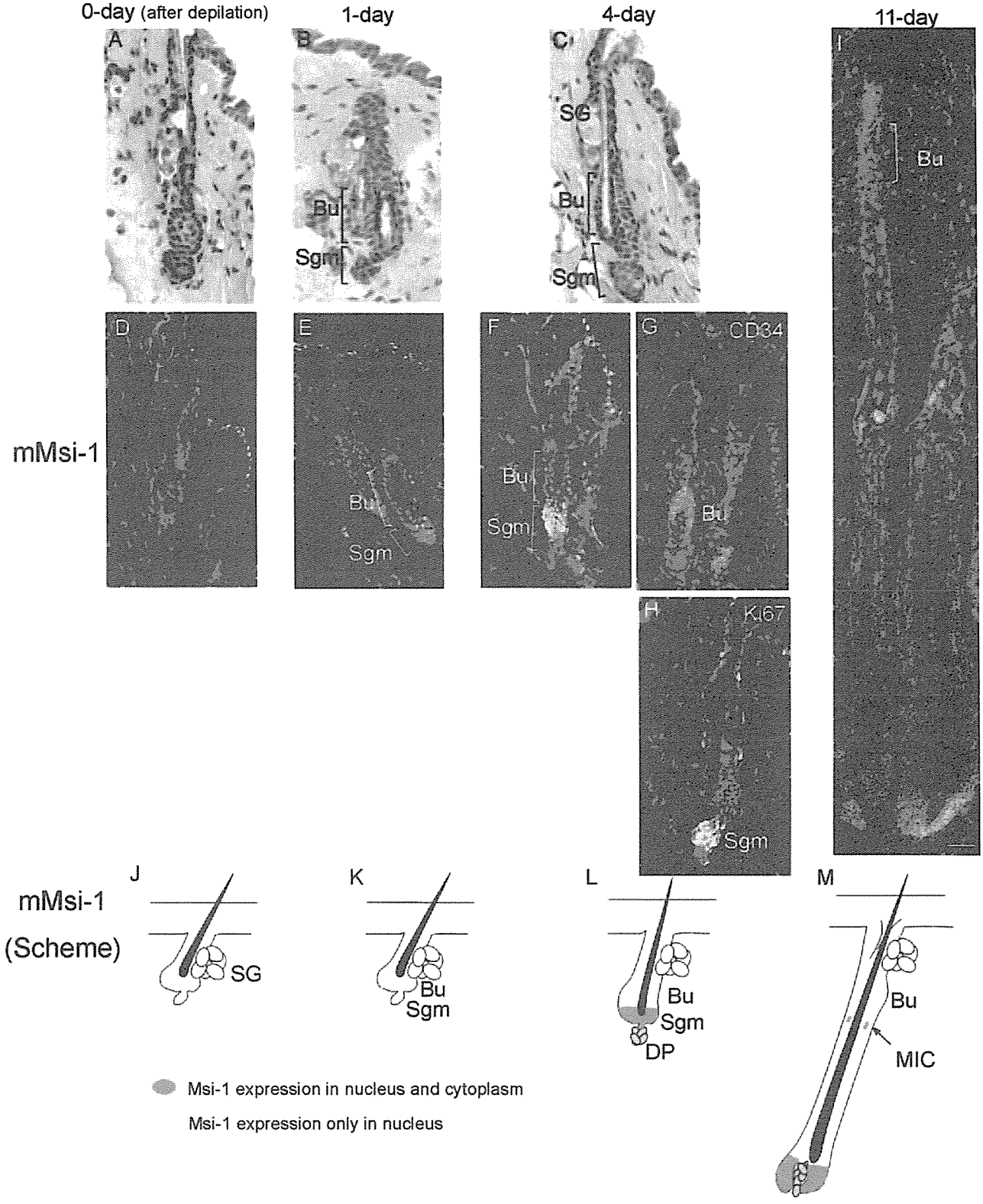

Figure 4. Msi-1 expression in the adult hair cycle of mice. Dorsal skin samples from 8-week-old C57BL/6 mice were harvested on days 0, 1, 4, and 11 after anagen induction. Sections were H&E stained (**A–C**) or processed for immunofluorescence staining with the anti-Msi-1 antibody (**D–F** and **I**), anti-CD34 antibody (**G**) or anti-Ki67 antibody (**H**). **D** and **J:** Msi-1 was not detected in HF at telogen. **E**, **F**, **K**, and **L:** After anagen induction, Msi-1 was expressed in the bulge and the secondary germ cells at early anagen. **I** and **M:** At late anagen, Msi-1 was expressed in MICs and the matrix cells, although the bulge cells were completely devoid of Msi-1 expression. **A**, **D**, and **J:** Day 0 after depilation (telogen); **B**, **E**, and **K:** 1 day after depilation (anagen); **C**, **F–H**, and **L:** 4 days after depilation (anagen); **I** and **M:** 11 days after depilation (anagen). **G:** Expression of CD34 in mice HF 4 days after depilation. **H:** Expression of Ki67 in mice HFs 4 days after depilation. **J–M:** Schematic representation of immunoreactivity patterns of Msi-1 during murine adult hair cycle. Green shows Msi-1 expression in nucleus and cytoplasm. Yellow shows Msi-1 expression only in nucleus. SG, sebaceous gland; Bu, bulge; DP, dermal papilla; MIC, middle IRS cells. Scale bar, 50 μm.

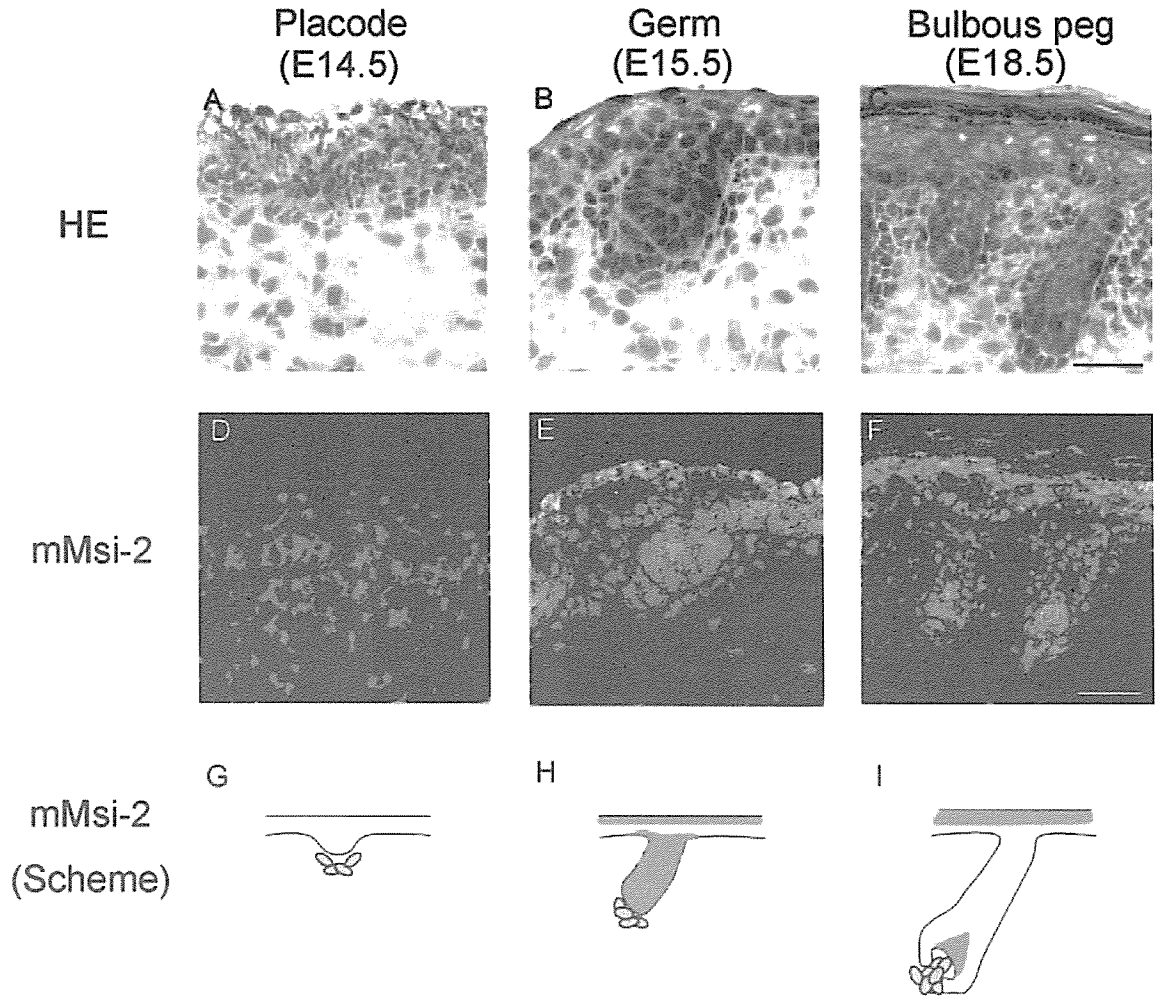

Figure 5. Msi-2 was expressed in mouse embryonic skin. C57BL/6 mouse back skin samples at the following developmental stages (E14.5, E15.5, and E18.5) were processed for immunohistological analysis of Msi-2. Sections were stained for H&E (**A–C**) or indirect immunofluorescence staining with the anti-Msi-2 antibody (**D–F**), in which Msi-2 fluorescence (green, FITC) and nuclear stain (red, propidium iodide) were merged. Msi-2 was not detected in undifferentiated epidermis at E14.5. At E15.5 and after, Msi-2 was expressed in the hair germ and the bulbous hair peg at developmental stages. **A**, **D**, and **G**, at E14.5; **B**, **E**, and **H**, at E15.5; **C**, **F**, and **I**, at E18.5. **G–I:** Schematic representation of immunoreactivity patterns of Msi-2 during murine embryonic epidermal development. Green color shows Msi-2 expression in both the nucleus and cytoplasm. Scale bars, 50 μm.

stages of fetal development until adulthood. In the transition from telogen to anagen phase, Msi-1 and Msi-2 were both expressed in the bulge region, a putative site rich in stem cells, and in the secondary germ cells, comprising early progenitor cells derived from the putative bulge stem cells. Moreover, during anagen phase, Msi-1 was also expressed in the matrix cells. The cells lie in the bulge region and are normally quiescent, but they are activated during early anagen and rapidly give rise to cycling transit-amplifying (TA) cells.[8,27] Thus, cells forming the secondary hair germ and the matrix are thought to be early progenitors of HF stem cells. Considering these facts, these Msi-positive cells may represent progenitor cells, or HF stem cells, supporting previously reported models.[14–16,18,22,23] In humans, Msi-1 mRNA and protein were detected in cultured keratinocytes, and Msi-1 protein was expressed in developing HFs, although we failed to detect this immunoreactivity in human adult skin.

In addition, Msi-1 was expressed in the outermost cell layers of the IRS in the mid-follicle, just below the IRS keratinization point (MIC), and Msi-2 was expressed throughout the entire IRS including MICs. MICs were confirmed not to contain BrdU label after 2 weeks of chase and are therefore not label-retaining cells. We thought that these MICs might lie in the Huxley layer of the IRS based on their location within the HF. Moreover, during HF development, Msi-2 was expressed in the cells that lie in the IRS cone that are the progenitor cells for the IRS. This localization pattern suggested that Musashi family proteins play some roles in IRS formation. RT-PCR analysis of the mRNA levels in mouse and human keratinocytes suggested that Musashi may work in both undifferentiated and differentiated keratinocytes. Considering these findings, Musashi family proteins are thought to have at least two roles in HF, ie, one associated with asymmetric division of the stem cell or early progenitor cell population and the other functioning during the differentiation of IRS cells.

In this study, we showed several differences between mouse and human Musashi expression in the skin. The

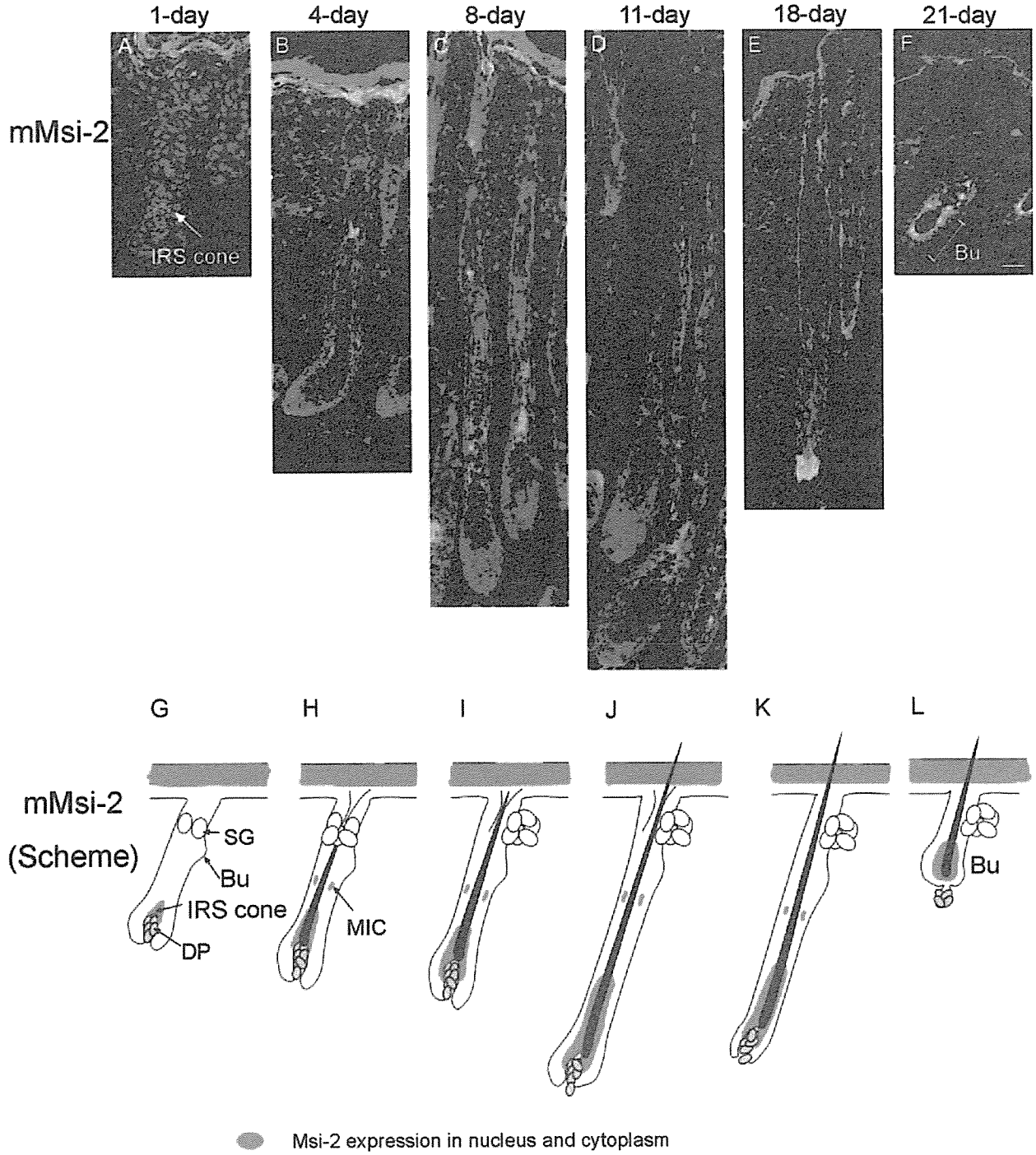

Figure 6. Msi-2 expression in the interfollicular epidermis and HF of neonatal mice. Dorsal skin samples from C57BL/6 newborn mice were harvested on days 1, 4, 8, 11, 18, and 21 after birth. **A** and **G:** Msi-2 was expressed in IRS cone (preIRS cells) at 1 day. **B–E** and **H–K:** From anagen to early catagen phases, Msi-2 was expressed in IRS cells and MICs. **F** and **L:** The transition from telogen to early anagen phase, Msi-2 was expressed in the bulge cells. **A** and **G**, 1-day-old (anagen); **B** and **H**, 4-day-old (anagen); **C** and **I**, 8-day-old (anagen); **D** and **J**, 11-day-old (anagen); **E** and **K**, 18-day-old (early catagen); **F** and **L**, 21-day-old mice (transition from telogen to anagen state). **G–L:** Schematic representation of Msi-2 immunoreactivity patterns in murine neonatal skin. Green indicates Msi-2 expression in nucleus and cytoplasm. SG, sebaceous gland; Bu, bulge; DP, dermal papilla; MIC, middle IRS cells. Scale bar, 50 μm.

discrepancy in the expression pattern of Musashi family proteins has also been observed in other tissues.[23] Although the exact reasons remain unclear, we believe this Msi-1 and Msi-2 expression discrepancy between mouse and human keratinocytes is mainly due to the fact that only Msi-1 has been identified in humans although both Msi-1 and Msi-2 have been identified in mice. Thus, Msi-1 may serve concurrently as Msi-2 in certain functions in humans.

An additional reason for the discrepancy in Msi-1 and Msi-2 expression is that the manner in which HF development and hair cycle progression takes place are quite different between the mouse and human. In mice,

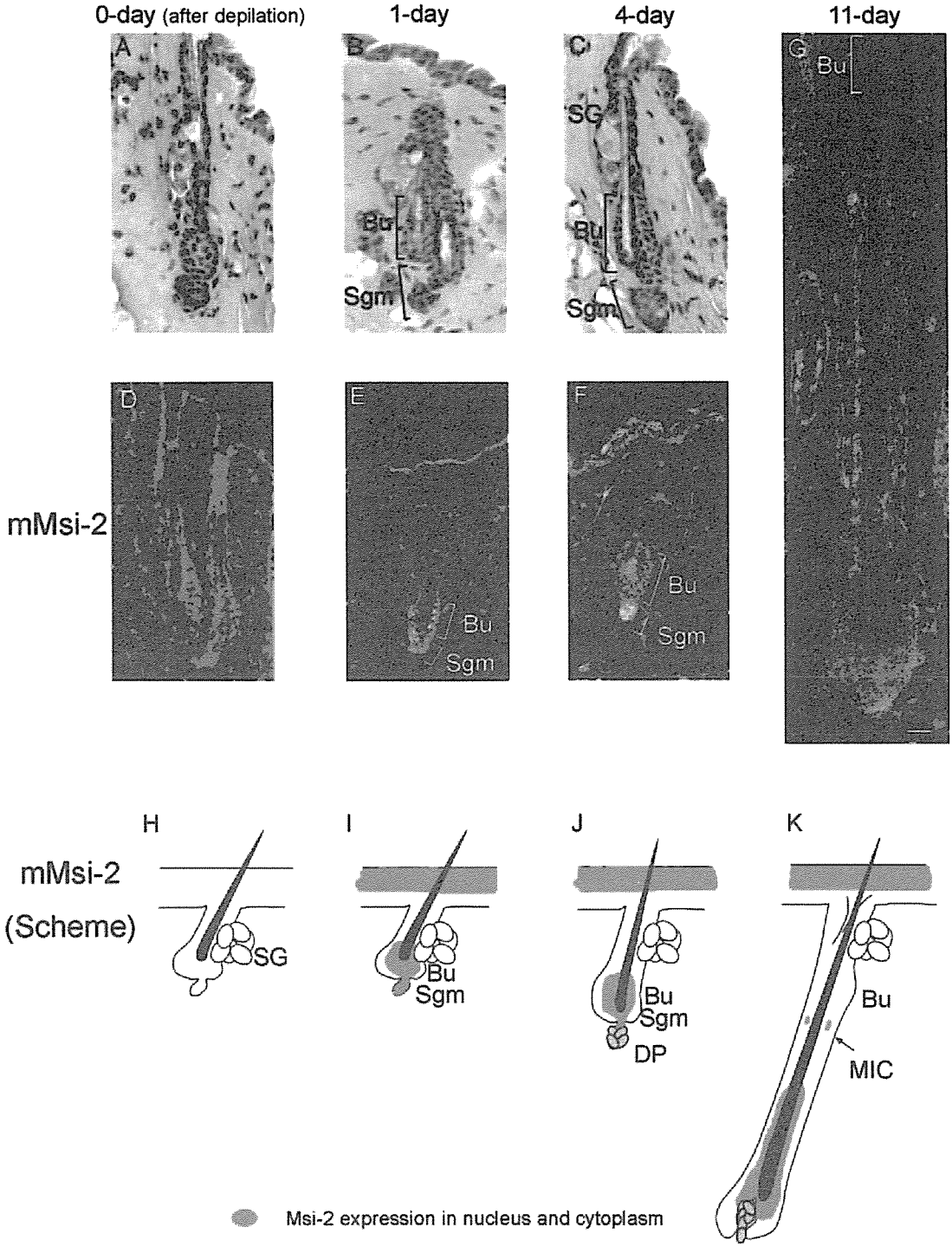

Figure 7. Msi-2 expression during the mouse adult hair cycle. Dorsal skin samples from 8-week-old C57BL/6 mice were harvested on days 0, 1, 4, and 11 after anagen induction. Sections were subjected to H&E staining (**A–C**) or immunofluorescence staining with the anti-Msi-2 antibody (**D–G**). **D** and **H:** Msi-2 was not detected at telogen phase. **E**, **F**, **I**, and **J:** After anagen induction, Msi-2 was expressed in the bulge and the secondary germ cells. **G** and **K:** At late anagen, Msi-2 was expressed in IRS cells and MICs, although bulge cells were completely devoid of Msi-1 expression. **A**, **D**, and **H**, day 0 after depilation (telogen); **B**, **E**, and **I**, 1 day after depilation (anagen); **C**, **F**, and **J**, 4 days after depilation (anagen); **G** and **K**, 11 days after depilation (anagen). **H–K:** Schematic representation of Msi-2 immunoreactivity patterns during the murine adult hair cycle. Green shows Msi-2 expression in nucleus and cytoplasm. SG, sebaceous gland; Bu, bulge; DP, dermal papilla; MIC, middle IRS cells. Scale bar, 50 μm.

Msi-1 and Msi-2 were expressed in the bulge and secondary hair germ cells that are thought to be putative stem and early progenitor cells. However, we failed to detect Musashi expression in the corresponding regions in the human HF. This discrepancy may be related to differences in the hair cycles: in mice the hair cycle is synchronized whereas in humans it is not synchronized and is more random.

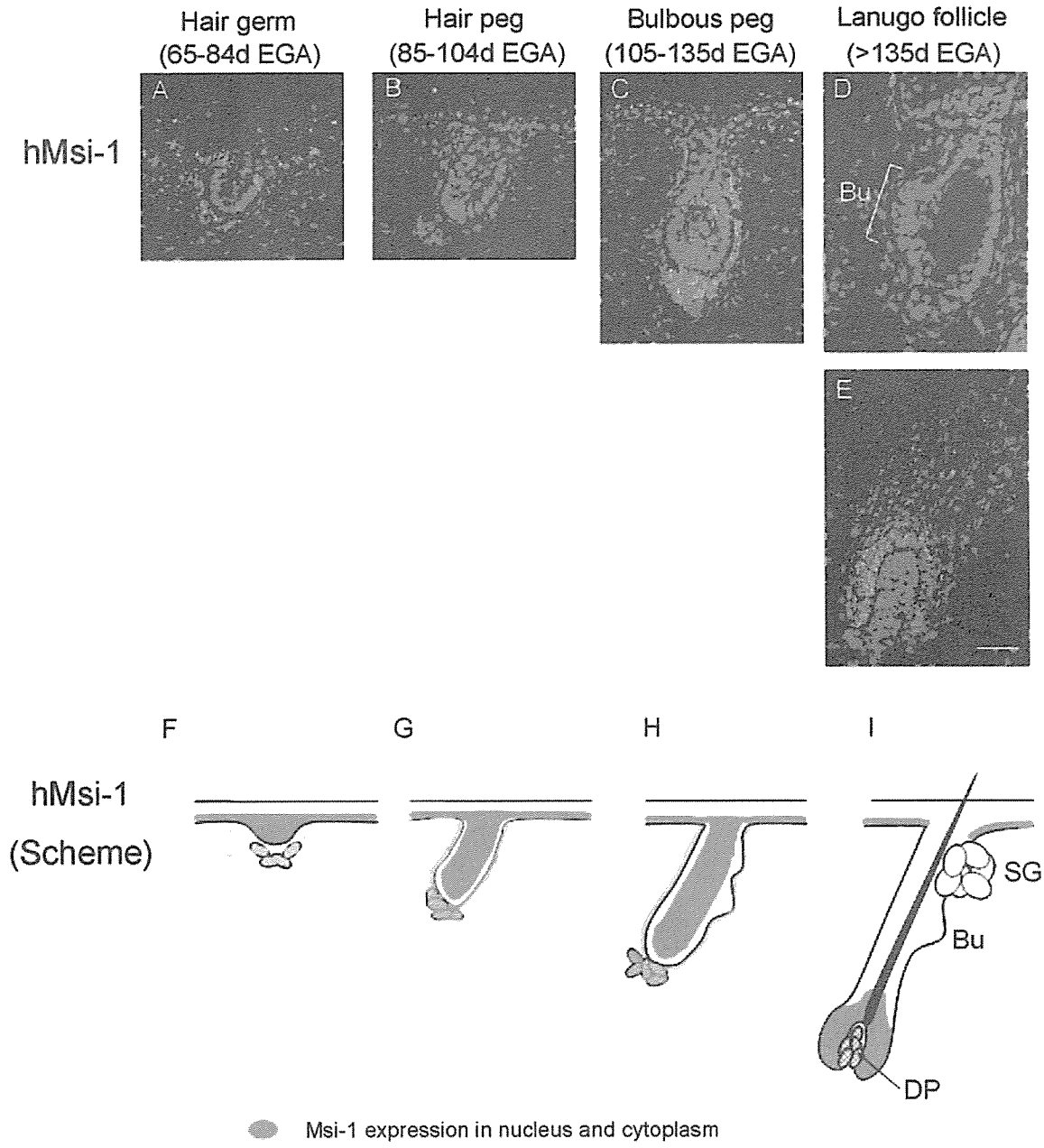

Figure 8. Msi-1 expression during human skin development. Human embryonic and fetal skin specimens were obtained from abortuses of 49 to 163 days EGA and subjected to indirect immunofluorescence analysis. Msi-1 was expressed in the hair germ (**A**, **F**), peg (**B**, **G**), and bulbous peg (**C**, **H**). In the lanugo HF (**D**, **E**, **I**), Msi-1 was expressed only in matrix cells, and the bulge cells were devoid of Msi-1 expression. **F**, **G**, **H:** Throughout human skin development, Msi-1 was expressed in the dermal cells surrounding developing HFs. **A** and **F**, hair germ cells (65 to 84 days EGA); **B** and **G**, hair peg cells (85 to 104 days EGA); **C** and **H**, early bulbous peg (108 days EGA); **D** and **I**, bulge cells of the lanugo HF (>135 days EGA); **E** and **I**, matrix cells of the lanugo HF (>135 days EGA). **F–I:** Schematic representation of the Msi-1 immunoreactivity pattern during human skin development. Green highlights Msi-1 expression in the nucleus and cytoplasm. SG, sebaceous gland; Bu, bulge; DP, dermal papilla. Scale bar, 50 μm.

Both Msi-1 and Msi-2 are RNA-binding proteins characterized by two RNP-type RNA recognition motifs (RRMs) that show a remarkable similarity to each other, both in their primary structures and their RNA-binding specificities.[14–16] Msi-1 and Msi-2 are known to be predominantly co-expressed in proliferating embryonic pluripotent neural precursors,[14–16] and disruption of either the *Msi-1* or *Msi-2* genes alone shows no effect on the number or self-renewal activity of the central nervous system stem cells.[20] Considering these facts, Msi-1 and Msi-2 may be able to compensate for the loss of the other in mice.

Several molecules are suggested to be regulated at the translational level by Musashi family proteins in the epidermis and HF. Msi-1 is a positive regulator of Notch-signaling through its interaction with *m-Numb* mRNA.[21] Notch-1, a large transmembrane receptor, is expressed in the developing or differentiating epidermis and HF.[28,29] Notch-1 is also known to initiate epidermal ter-

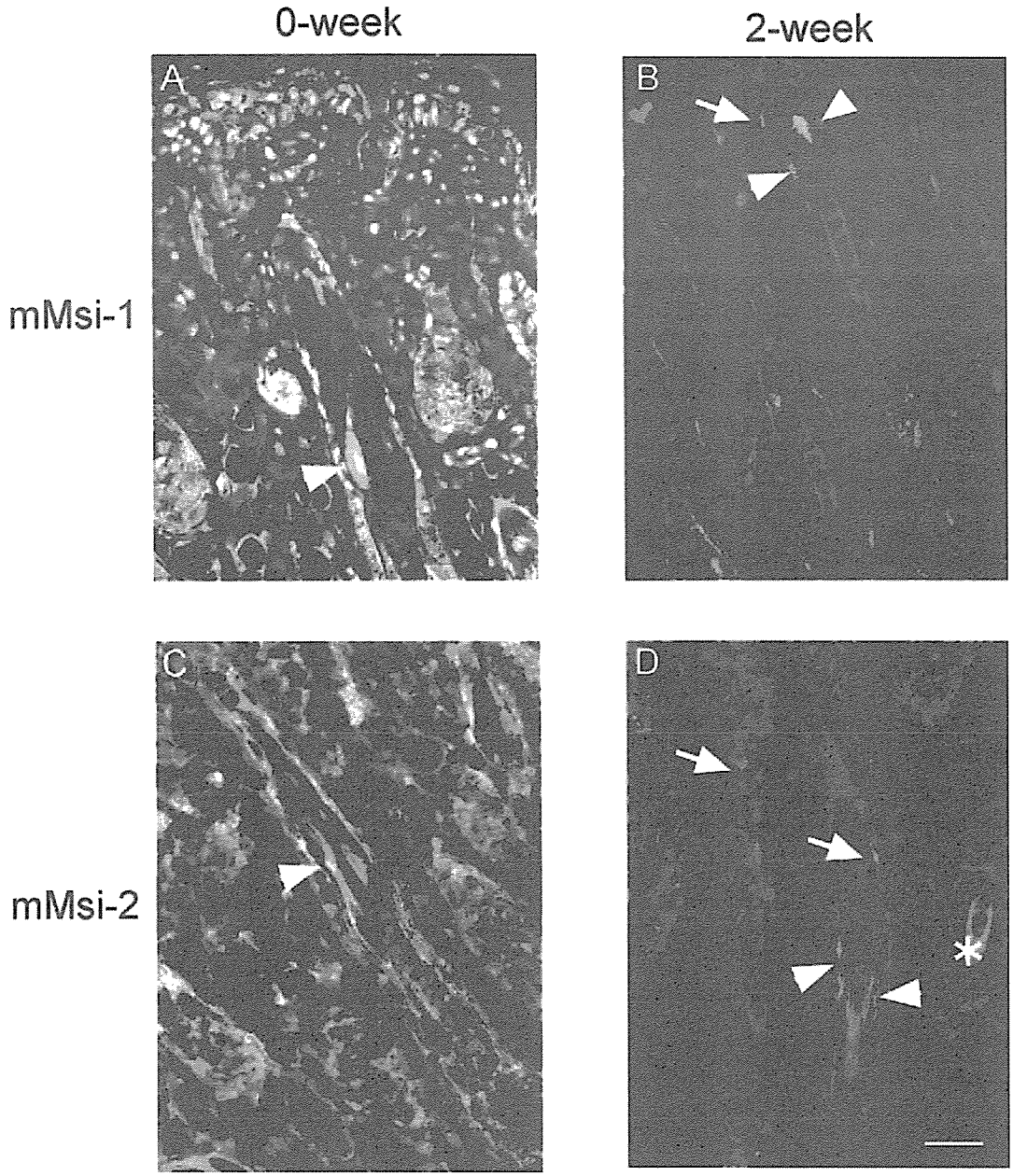

Figure 9. Musashi-positive HF epithelial cells in neonatal mice are not slow-cycling cells. To detect slow-cycling cells (putative stem cells), BrdU (50 μg/g body weight) was injected into neonatal C57BL/6J mice from day 3 after birth, twice a day for 3 days. Musashi-positive MICs were also BrdU-positive (**A**, **C**; **arrowheads**) immediately after BrdU injection, although after a 2-week chase MICs (**B**, **D**; **arrowheads**) were not BrdU-positive. Cells retaining the label after 2 weeks (**B**, **D**; **arrows**) were identified as slow-cycling cells. Neither Msi-1-positive cells (**B**, **arrowheads**) nor Msi-2-positive cells (**D**, **arrowheads**) were slow-cycling cells. **A** and **C**, 0 day after labeling; **B** and **D**, 2 weeks after labeling. Green (FITC), Msi-1 (**A**, **B**), or Msi-2 (**C**, **D**); red (tetramethyl-rhodamine isothiocyanate), BrdU; blue (TOPRO), nuclear staining. **Asterisk** indicates nonspecific staining. Scale bar, 50 μm.

minal differentiation and regulate HF differentiation, especially in IRS cell lineages.[30,31] In our study, we showed that Msi-1 was expressed in the epidermis, the entire hair germ, and inner cells of the hair peg of mice and humans during HF development. This distribution of Msi-1 during HF development is similar to that of Notch-1.[28,29] Notch-1 is expressed in the inner cells of the embryonic placode and the follicle bulb cells where it is thought to determine cell fate.[28,29] Moreover, Msi-1 was expressed in matrix cells during anagen phase in which Notch-1 was also expressed in the anagen HF. Considering these expression patterns, regulators of the Notch signaling pathway, including m-Numb, are potential targets for Musashi proteins in the HF, although Msi-1 and Msi-2 may work in different ways from those proposed for the other tissues.

Previous studies that identified the RNA sequences targeted by Msi-1 showed that Msi-1 could bind poly(G) and poly(U) RNA *in vitro*[14] and could also bind to UG-rich sequences [(G/A)UnAGU] using SELEX.[21] Msi-1 may also bind gene sequences other than m-Numb to promote HF morphogenesis and control the hair cycle. Indeed, several molecules that contribute to development and progression of HF, including β-catenin, fibroblast growth factor-5, transforming growth factor-β2, BMP-2,

Sonic Hedgehog, and others,[1] have this UG-rich consensus sequence. Further studies are needed to identify Musashi mRNA targets in HFs.

In this study, Msi-1 protein expression was mostly cytoplasmic. However, in some instances, nuclear staining was seen in interfollicular epidermal and HF cells. The reasons for these altered expression patterns, with both cytoplasmic and nuclear distributions, remain unclear, although similar variations in Msi-1 subcellular localization have been reported in other tissues.[23] Msi-1 localizes to the nucleus in epithelial cells, and Msi-1 possesses a potential phosphorylation site for cdc-2 kinase, a cyclin-dependent kinase that can bind cyclin B and regulate mitosis. Thus, Msi-1 may be posttranslationally modified in the nucleus during specific phases of the cell cycle.

In summary, Msi-1 and Msi-2 proteins were expressed in the HF and epidermis from the earliest developmental stage examined until adulthood in mice whereas only Msi-1 was expressed in the developing human HF. Msi-1 and Msi-2 expression was restricted to the bulge, secondary hair germ, and IRS cells, including MIC. These results suggest that Msi-1 and Msi-2 play important roles in HF development and progression of the hair cycle by regulating asymmetric cell division and the differentiation of IRS cells.

Acknowledgments

We thank Mrs. Megumi Sato and Ms. Kaori Sakai for their technical assistance and Dr. James R. McMillan for his critical reading of this manuscript.

References

1. Schmidt-Ullrich R, Paus R: Molecular principles of hair follicle induction and morphogenesis. Bioessays 2005, 27:247–261
2. Cotsarelis G, Sun TT, Lavker RM: Label-retaining cells reside in the bulge area of pilosebaceous unit: implications for follicular stem cells, hair cycle, and skin carcinogenesis. Cell 1990, 61:1329–1337
3. Lavker RM, Cotsarelis G, Wei ZG, Sun TT: Stem cells of pelage, vibrissae, and eyelash follicles: the hair cycle and tumor formation. Ann NY Acad Sci 1991, 642:214–224
4. Lavker RM, Miller SJ, Sun TT: Epithelial stem cells, hair follicles, and tumor formation. Recent Results Cancer Res 1993, 128:31–43
5. Sun TT, Cotsarelis G, Lavker RM: Hair follicular stem cells: the bulge-activation hypothesis. J Invest Dermatol 1991, 96:77S–78S
6. Kobayashi K, Rochat A, Barrandon Y: Segregation of keratinocyte colony-forming cells in the bulge of the rat vibrissa. Proc Natl Acad Sci USA 1993, 90:7391–7395
7. Rochat A, Kobayashi K, Barrandon Y: Location of stem cells of human hair follicles by clonal analysis. Cell 1994, 76:1063–1073
8. Taylor G, Lehrer MS, Jensen PJ, Sun TT, Lavker RM: Involvement of follicular stem cells in forming not only the follicle but also the epidermis. Cell 2000, 102:451–461
9. Oshima H, Rochat A, Kedzia C, Kobayashi K, Barrandon Y: Morphogenesis and renewal of hair follicles from adult multipotent stem cells. Cell 2001, 104:233–245
10. Morris RJ, Liu Y, Marles L, Yang Z, Trempus C, Li S, Lin JS, Sawicki JA, Cotsarelis G: Capturing and profiling adult hair follicle stem cells. Nature Biotechnol 2004, 22:411–417
11. Tumbar T, Guasch G, Greco V, Blanpain C, Lowry WE, Rendl M, Fuchs E: Defining the epithelial stem cell niche in skin. Science 2004, 303:359–363
12. Blanpain C, Lowry WE, Geoghegan A, Polak L, Fuchs E: Self-renewal, multipotency, and the existence of two cell populations within an epithelial stem cell niche. Cell 2004, 118:635–648
13. Nakamura M, Okano H, Blendy JA, Montell C: Musashi, a neural RNA-binding protein required for Drosophila adult external sensory organ development. Neuron 1994, 13:67–81
14. Sakakibara S, Imai T, Hamaguchi K, Okabe M, Aruga J, Nakajima K, Yasutomi D, Nagata T, Kurihara Y, Uesugi S, Miyata T, Ogawa M, Mikoshiba K, Okano H: Mouse-Musashi-1, a neural RNA-binding protein highly enriched in the mammalian CNS stem cell. Dev Biol 1996, 176:230–242
15. Sakakibara S, Okano H: Expression of neural RNA-binding proteins in the postnatal CNS: implications of their roles in neuronal and glial cell development. J Neurosci 1997, 17:8300–8312
16. Sakakibara S, Nakamura Y, Satoh H, Okano H: RNA-binding protein Musashi2: developmentally regulated expression in neural precursor cells and subpopulations of neurons in mammalian CNS. J Neurosci 2001, 21:8091–8107
17. Good P, Yoda A, Sakakibara S, Yamamoto A, Imai T, Sawa H, Ikeuchi T, Tsuji S, Satoh H, Okano H: The human Musashi homolog 1 (MSI1) gene encoding the homologue of Musashi/Nrp-1, a neural RNA-binding protein putatively expressed in CNS stem cells and neural progenitor cells. Genomics 1998, 52:382–384
18. Kaneko Y, Sakakibara S, Imai T, Suzuki A, Nakamura Y, Sawamoto K, Ogawa Y, Toyama Y, Miyata T, Okano H: Musashi1: an evolutionally conserved marker for CNS progenitor cells including neural stem cells. Dev Neurosci 2000, 22:139–153
19. Okano H, Imai T, Okabe M: Musashi: a translational regulator of cell fate. J Cell Sci 2002, 115:1355–1359
20. Sakakibara S, Nakamura Y, Yoshida T, Shibata S, Koike M, Takano H, Ueda S, Uchiyama Y, Noda T, Okano H: RNA-binding protein Musashi family: roles for CNS stem cells and a subpopulation of ependymal cells revealed by targeted disruption and antisense ablation. Proc Natl Acad Sci USA 2002, 99:15194–15199
21. Imai T, Tokunaga A, Yoshida T, Hashimoto M, Mikoshiba K, Weinmaster G, Nakafuku M, Okano H: The neural RNA-binding protein Musashi1 translationally regulates mammalian numb gene expression by interacting with its mRNA. Mol Cell Biol 2001, 21:3888–3900
22. Kayahara T, Sawada M, Takaishi S, Fukui H, Seno H, Fukuzawa H, Suzuki K, Hiai H, Kageyama R, Okano H, Chiba T: Candidate markers for stem and early progenitor cells, Musashi-1 and Hes1, are expressed in crypt base columnar cells of mouse small intestine. FEBS Lett 2003, 535:131–135
23. Potten CS, Booth C, Tudor GL, Booth D, Brady G, Hurley P, Ashton G, Clarke R, Sakakibara S, Okano H: Identification of a putative intestinal stem cell and early lineage marker; Musashi-1. Differentiation 2003, 71:28–41
24. Sakatani T, Kaneda A, Iacobuzio-Donahue CA, Carter MG, Witzel SB, Okano H, Ko MSH, Ohlsson R, Longo DL, Feinberg AP: Loss of imprinting of Igf 2 alters intestinal maturation and tumorigenesis in mice. Science 2005, 307:1976–1978
25. Akasaka Y, Saikawa Y, Fujita K, Kubota T, Ishii T, Okano H, Kitajima M: Expression of a candidate marker for progenitor cells, Musashi-1, in the proliferative regions of human antrum and its decreased expression in intestinal metaplasia. Histopathology 2005, 47:348–356
26. Clarke RB, Spence K, Anderson E, Howell A, Okano H, Potten CS: A putative human breast stem cell population is enriched for steroid receptor-positive cells. Dev Biol 2005, 277:443–456
27. Wilson C, Cotsarelis G, Wei ZG, Fryer E, Margolis-Fryer J, Ostead M, Tokarek R, Sun TT, Lavker RM: Cells within the bulge region of mouse hair follicle transiently proliferate during early anagen: heterogeneity and functional differences of various hair cycles. Differentiation 1994, 55:127–136
28. Powell BC, Passmore EA, Nesci A, Dunn SM: The Notch signalling pathway in hair growth. Mech Dev 1998, 78:189–192
29. Favier B, Fliniaux I, Thelu J, Viallet JP, Demarchez M, Jahoda CA, Dhouailly D: Localisation of members of the notch system and the differentiation of vibrissa hair follicles: receptors, ligands, and fringe modulators. Dev Dyn 2000, 218:426–437
30. Lin MH, Leimeister C, Gessler M, Kopan R: Activation of the Notch pathway in the hair cortex leads to aberrant differentiation of the adjacent hair-shaft layers. Development 2000, 127:2421–2432
31. Yamamoto N, Tanigaki K, Han H, Hiai H, Honjo T: Notch/RBP-J signaling regulates epidermis/hair fate determination of hair follicular stem cells. Curr Biol 2003, 13:333–338

Gene Therapy (2006) 13, 732–737

www.nature.com/gt

SHORT COMMUNICATION

Hair follicle stem cell-targeted gene transfer and reconstitution system

Y Sugiyama-Nakagiri, M Akiyama and H Shimizu
Department of Dermatology, Hokkaido University Graduate School of Medicine, Sapporo, Japan

Gene transfer to hair follicle (HF) epithelium is an attractive approach for not only treating skin diseases, but also many systemic disorders. In this study, we attempted to develop a gene transfer system for HF epithelial stem cells to maximize the beneficial therapeutic effects. For persistent and stable transgene expression in HF stem cells, we transferred retroviral vectors encoding reporter genes into cultured HF stem cells. In addition, these cells were mixed with cultured dermal papilla cells and transplanted on to immunodeficient mice. We succeeded in reconstituting HFs and their appendages in which these cells harbored a transgene reporter. The transgene expression was observed in all skin epithelial compartments including the HF epithelium, sebaceous gland and epidermis. In addition, transgene expression was observed for at least 6 months. This HF stem cell-targeted gene transfer and reconstitution system provides reliable gene-function analysis and gene therapy.
Gene Therapy (2006) **13,** 732–737. doi:10.1038/sj.gt.3302709; published online 5 January 2006

Keywords: *bulge; gene transfer; hair follicle; reconstitution; stem cell*

Hair follicle (HF) epithelium is an ideal target for gene therapy for many systemic diseases as well as skin disorders, because HFs are located at the surface of the body and are readily accessible without causing undue damage to the integument. In addition, HFs have an obvious potential to be used to produce local and systemic proteins.

To establish a therapeutic gene transfer system for HFs, many researchers have tried using a variety of methods.[1–5] Intradermal injection of purified DNA, topical application of liposome–DNA complexes, high pressure gene gun and virus infection have been used to transfer genes into HFs. In order to obtain stable and persistent transgene expression and maximize the beneficial transgene therapeutic effects, the stem cell population should preferentially be targeted.

The HF stem cells have been reported to lie in the HF bulge region.[6–9] Many cells derived from the bulge contain colony-forming cells,[10,11] and have a slow cycling, quiescent nature.[12] Transplantation studies and bromodeoxyuridine (BrdU) labeling experiments suggest that bulge cells possess the ability to differentiate into any kind of cutaneous epithelial cell, including the sebaceous gland and interfollicular epidermal keratinocytes.[12–16]

The final goal of this study was to develop an efficient gene transfer system targeted for skin epithelial stem cells located in the bulge region. To establish optimal, persistent and stable expression of the transgene, a recombinant retroviral system was adopted because of its high gene transfer and integration efficiency,[17] although the transduction of retrovirus vector requires cells to be undergoing replication at the time of infection.[18] Thus, it has been difficult to introduce genes directly into the stem cells *in vivo*, because the stem cell population in the HF epithelium and the epidermis is a relatively small population and stem cells are relatively slowly cycling.[12]

At first, we established a HF stem cell-rich culture system using cells from rat vibrissa bulge cells (Figure 1a) and evaluated the nature of these cells. *In vitro*, primary cultures of bulge-derived cells formed significantly more colonies than arose from outer root sheath cells (ORS) (Figure 1b) as has been described previously.[10] Furthermore, the proliferation rate of cells from the bulge in long-term culture was greater than that of ORS cells (Figure 1c) and bulge-derived cells retained the ability to form colonies after three passages. These results confirmed the previous report[16] that bulge-derived cells display self-renewal characteristics of stem cells even if they are removed from their native niche and induced to proliferate in culture.

In order to obtain transcriptional profiles of bulge-derived cells, we carried out microarray analysis (Figure 1d and Supplementary Table 1). In stem cell-rich cultures from the bulge, 78 mRNA species were upregulated more than twofold, and 88 mRNA species were downregulated more than twofold in comparison with cultured ORS cells. Stem cell-rich bulge-derived cells showed upregulated expression of several genes including, *Col2a1*, *Igfbp3*, *Igfbp6* and *Fgf13*, which have been already reported to be upregulated in stem cells in the previous reports (Figure 1d).[14–16] These results further confirmed that cultured bulge-derived cells contained the HF stem cell population. In the present study, none of CD34, β1-integrin or S100a4, all of which were reported

Correspondence: Dr M Akiyama, Department of Dermatology, Hokkaido University Graduate School of Medicine, North 15 West 7, Sapporo 060-8638, Japan.
E-mail: akiyama@med.hokudai.ac.jp
Received 30 August 2005; revised 15 November 2005; accepted 18 November 2005; published online 5 January 2006

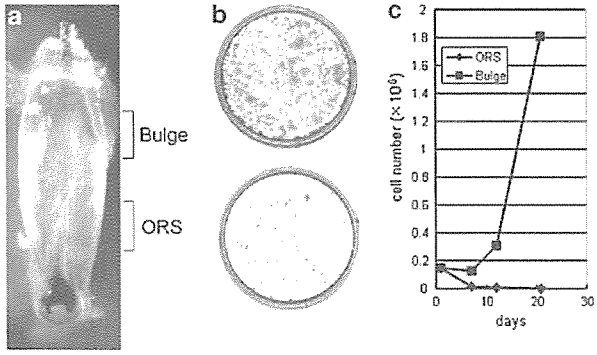

d Selected genes whose expression were up-regulated in HF bulge cells

Gene name/protein name	Fold higher expression
Procollagen, type II, alpha 1*	8.65
Insulin-like growth factor binding protein 3*	6.03
matrix metalloproteinase 3	6.03
ornithine decarboxylase 1	3.49
Insulin-like growth factor binding protein 6*	2.91
transforming growth factor, alpha	2.80
Fibroblast growth factor 13*	2.71
EphA7	2.40
follistatin	2.09
peroxiredoxin 3	2.08

Figure 1 Characterization of cultured bulge cells. (**a**) A HF was isolated from rat vibrissa. Rats or mice were killed by carbon dioxide asphyxiation. The upper lip containing the two vibrissa pads were cut out and its inner surface was exposed. Each selected vibrissa was then microdissected under a binocular microscope. The subcutaneous fat and connective tissue surrounding the vibrissa capsule was then carefully removed. The vibrissa was then pulled away from the pad by holding its neck with fine forceps. (**b**) The growth of bulge-derived cell colonies (upper) and outer root sheath (ORS) cell colonies (lower) from rat vibrissa. The follicle was cut into four fragments. From the bulbar side, the first transverse cut was made just above the hair bulb, and the second was made at the site of insertion of the nerve fibers, which is proximal to the site of inferior enlargement of the outer sheath. The third cut was made just below the sebaceous glands. The lower part of the capsule was then carefully prized away from the bulb; special care was taken at this stage to leave the dermal papilla in place. ORS cells were isolated from second lowest part and bulge cells were isolated from third lower part of the vibrissa follicles. Each fragment was then transferred into dispase solution (Godoshusei Ltd) and was incubated for 1 h at 4°C. The epithelial cells were then teased away from the thin dermal sheath with fine needles. A 0.25% solution of trypsin was then added and the cell and HF fragments were further incubated for 10 min at 4°C. Equal numbers of live cells were plated onto mitomycin C-treated 3T3 fibroblasts in Defined-Keratinocyte Serum Free Medium (Invitrogen). The cells were cultured for 1 week *in vitro* and either fixed and stained with Rhodamine B for visual inspection or; (**c**) passaged for long term survival and growth analysis. (**d**) Selected genes whose expression was upregulated in HF bulge cells. For microarray analysis, isolated cultured cells derived from rat vibrissae bulge or ORS were collected. We used 5 μg of total RNA from each cell population as a starting material, and no amplification steps beyond mRNA transcription were performed to minimize the chance of losing accurate representations of mRNA levels. The mRNA products were hybridized to a Rat oligo microarray (Agilent). All protocols and data analysis were conducted according to the manufacturer's manual. The genes whose upregulated expression had been reported previously were denoted by asterisks (*).

previously as HF stem cell markers,[14–16] was upregulated in bulge-derived cells. These differences might be caused by different states that the putative stem cells are maintained in. Thus, the putative stem cell markers, CD34, β1-integrin and S100a4, may be associated with stem cells in a quiescent state in the bulge niche. Conversely, genes that were upregulated in both quiescent and proliferating states may prove to be better marker molecules for stem cells in their proliferate state.

Subsequently, we regenerated an entire HF epithelium and interfollicular epidermis using cultured bulge-derived cells. The cultured bulge-derived cells including HF stem and progenitor cells were thoroughly mixed with neonatal rat vibrissa dermal papilla (DP) cells and this cell slurry engrafted into a silicone chamber implanted on to the backs of SCID mice as previously reported.[19] At 4 weeks after transplantation, the grafts containing bulge and DP cell mixtures exhibited tufts of hairs as well as complete interfollicular epidermis (Figure 2a).

To evaluate whether the reconstituted skin and appendages were truly derived from bulge cells, we grafted the bulge cells from vibrissa of adult Rosa 26 mice that constitutively express the *lacZ* reporter gene under the control of an SV40 promoter, mixed with rat DP cells. The graft was harvested after 4 weeks and then stained for β-galactosidase. The entire epithelium including HF, sebaceous gland and the interfollicular epidermis was β-galactosidase-positive and the DP cells were completely devoid of β-galactosidase staining (Figure 2b). These results indicated that the cultured cells derived from the bulge region retained their multipotent potential to create multiple epithelial skin and appendages (Figure 2c). In addition, adult tissue-derived cells also maintained this ability.

Hematoxylin and eosin (H&E) staining of frozen sections of reconstituted HFs showed that the morphology of the reconstituted HFs was very similar to that of normal rat pelage follicles (Figure 2d), although the dermis was more tightly packed with fibroblasts than is usually seen in normal rat skin. The reconstituted HFs were also randomly orientated in contrast to the uniform orientation of normal skin (data not shown).

Scanning electron microscopic observation of the reconstituted hairs revealed that the hair cuticle pattern was similar to that of normal rat vibrissa from where the cells were initially derived (Figure 2e and f), although reconstituted hairs were thinner than normal ones. Transmission electron microscopic observation revealed normal morphology of HFs. The reconstituted HFs displayed a normal inner root sheath (IRS), with sheath cuticle (Cs), Huxley's (Hu) and Henle's (He) layers readily identified by their electron-dense trichohyalin granules (Figure 2g) and an ORS (Figure 2h).

As a next step, we performed HF stem and progenitor cell-targeted gene transfer using a retrovirus vector with enhanced green fluorescent protein (EGFP) or *LacZ* as a marker. Cultured bulge-derived cells were infected with retrovirus carrying the EGFP gene, and 30–40% of cells expressed EGFP 4-days after infection (data not shown). EGFP-positive colonies were still observed after the third passage (Figure 3a). This result confirmed that the transgene had been successfully introduced into a subset of cells with a colony-forming ability (that were assumed to be putative stem cells).